RESEARCH ARTICLE

Response of Moisture and Temperature Diffusivity on an Orthotropic Hygro-thermo-piezo-elastic Medium

Vipin Gupta[1] · M. S. Barak[1] · Hijaz Ahmad[2,3,4] · Soumik Das[5] · Bandar Almohsen[6]

Abstract

This research explores the complex interaction between piezoelectric waves and heat-moisture diffusion within a semi-infinite piezoelectric material under hygro-thermal conditions. By employing a two-dimensional Cartesian framework, novel governing equations for a thermo-piezoelectrically orthotropic medium influenced by moisture effects are developed. Accurate representations for key parameters are obtained by utilizing normal mode analysis. The investigation examines the influence of critical factors like moisture content, diffusivity, and temperature diffusivity on the spatial distribution of various physical fields. Additionally, a particular scenario of significance is highlighted. These results have the potential to improve sensor, actuator, and energy-harvesting device performance and dependability.

List of symbols

$c_{ijkl} =$ Elastic stiffness tensor
$T =$ Thermal temperature
$q_i^F =$ Fourier's heat flux

✉ Hijaz Ahmad
hijaz.ahmad@neu.edu.tr

1   Department of Mathematics, Indira Gandhi University, Meerpur, Rewari, India

2   Near East University, Operational Research Center in Healthcare, TRNC Mersin 10, Nicosia, 99138, Turkey

3   Center for Applied Mathematics and Bioinformatics, Gulf University for Science and Technology, Mishref, Kuwait

4   Department of Computer Science and Mathematics, Lebanese American University, Beirut, Lebanon

5   School of Physical Sciences, Amrita Vishwa Vidyapeetham, Mysuru Campus, Mysore, Karnataka, India

6   Department of Mathematics, College of Science, King Saud University, P.O. Box 2455, 11451 Riyadh, Saudi Arabia

                                                      ∯ Springer

$q^d =$	Dufour flux
$\phi =$	Electrical potential
$\rho =$	Density
$\tau_i,\, d_i =$	Pyro-electric constants
$E_i =$	Electric field density
$q_{ij}^m =$	Coupled moisture diffusivities
$J =$	Moisture concentration potential
$D_{ij}^T =$	Temperature diffusivity
$a_{ij}^T =$	Coupling thermal material coefficients
$S =$	Entropy
$\beta_{ij}^T =$	Thermal moduli tensor
$e_{ij} =$	Component of strain
$f^F =$	Moisture flux
$f^s =$	Soret flux
$\eta_{ijr},\, \varepsilon_{ij} =$	Piezothermal moduli tensors
$D_i =$	Electric displacement
$C_E =$	Specific heat at constant strain
$\sigma_{ij} =$	Components of the stress
$Q_{ij}^T =$	Coupled thermal diffusivity
$K_m =$	Moisture diffusion constant
$D_{ij}^m =$	Moisture diffusivity
$\beta_{ij}^m =$	Moisture moduli tensor
$\delta_{ij} =$	Kroneckar delta

1 Introduction

Contemporary engineered materials, including composites, concrete, bio tissues, and foams, commonly exhibit susceptibility to heat and moisture due to their porous, fractured, and atomic structure. Piezoelectric materials are a category of intelligent materials that hold promise for enhancing network performance by employing active dampening, stiffening, and vibration mitigation [1]. However, thermal stresses caused by aerodynamic heating, heat transfer, and moisture transfer can lead to buckling, instability, and decreased stiffness and strength in these materials over their service life. As the temperature increases, fluid can be absorbed into the perforations, enlarging voids and tiny flaws and causing defects to expand. Conversely, when the temperature is lowered, trapped fluid can further broaden defects, resulting in potential system failure. Hence, the inclusion of the impact of hygro-thermal, highlighting the interplay between moisture and temperature, is crucial when scrutinizing the mechanical characteristics of these materials and structures[2]. Alhashash et al. [3] have presented a novel approach to understanding the behavior of semiconductor materials under the reference of the two-temperature hygro-thermo-elasticity theory. Alenazi et al. [4]conducted

research on the influence of moisture diffusivity in a semiconductor material within the framework of photo-thermoelasticity theory. El-Sapa et al. [5] delved into the study of moisture impact on the free surface of a semiconductor material. Their investigation utilized a one-dimensional deformation model to explore these interactions.

Piezoelectric materials are now widely used in many fields, such as medical imaging, energy harvesting, and vibration control. The term "piezoelectricity" describes the capability of certain crystals to generate a voltage when they are mechanically stressed, which can be used for various applications. The Curie brothers [6] were the first to discover this phenomenon, and their work laid the foundation for developing modern piezoelectric materials. Mindlin [7] developed an equation for the relationship between temperature and piezoelectric materials. The fundamental laws that govern thermo-piezo-elasticmaterials were explored by Nowacki [8, 9].In recent decades, there has been substantial progress made by researchers and engineers in enhancing the properties of piezoelectric materials, hence leading to an expansion of their potential uses. Numerous researchers [10–13] have conducted extensive research on wave propagation in different types of thermoelastic materials with piezoelectricity, diffusion, memory, and the two-temperature effect. Their findings have contributed significantly to understanding the behavior of plane waves in these mediums and finding practical applications in various fields, such as material engineering and acoustics. The energy transmission methods across several contact types, including elastic, thermo-elastic, and thermo-piezo-electric, have been thoroughly studied by Gupta and his team [14–22]. They have examined how numerous elements, including electric fields, phase delays, and memory derivatives, affect these energy transfer processes. This research holds significance in advancing the comprehension of interface behavior and in the development of novel applications in the realms of energy harvesting and vibration control. Gupta and his research team [23–25] conducted an in-depth investigation into diverse wave phenomena within a porous fiber-reinforced thermoelastic medium. Their study considered the influence of memory effects, magnetic fields, and nonlocality on the observed phenomena. Further research is necessary to understand how piezoelectric composite materials perform in hygro-thermal environments.

Hygro-piezo-thermo-elastic (HPTE) materials are of significant importance as they offer a diverse range of properties that can be customized to cater to specific engineering needs. The combination of mechanical, electrical, and hygro-thermal features makes these materials capable of actively reducing vibrations, enhancing stiffness and strength, and adapting to variations in temperature and humidity. Due to these exceptional characteristics, they have immense potential for applications in diverse fields, including aerospace, robotics, and environmental monitoring, where precise control over material properties is critical. Using the virtual work idea, Raja et al. [26] have demonstrated how active stiffness affects the dynamic behavior of HPTE laminates. Gupta et al. [27] carried out an extensive review, examining the impacts of hygro-thermal conditions and additional non-linear influences on the mathematical formulation of smart structures incorporating piezoelectric elements. This review provides valuable insights into the challenges and opportunities in developing more advanced and robust models for piezoelectric intelligent systems.

Zenkour and Alghanmi [28] investigated the behavior of sandwich plates under electro-mechanical-hygro-thermo sinusoidal loadings using piezoelectric material faces and a functionally graded core.

Tiwari and her research team [29–35] conducted an in-depth investigation into wave propagation, examining various scenarios, including continuous line heat sources, magneto-thermoelasticity, and memory-dependent derivatives. Their research yielded valuable insights into material behaviors under specific conditions, with implications for applications ranging from thermal management to high-temperature environments. Through the integration of memory-dependent phenomena and nonlocal effects, Tiwari's work contributes to the advancement of theoretical frameworks, offering support for material design and optimization in diverse technological domains. Kaur's research group [36–39] has significantly advanced the understanding of thermoelastic damping and dynamic responses in nanobeams, primarily focused on generalized piezothermoelastic nanobeams with simply supported boundaries. Additionally, they examined the magneto-electro-piezo-thermoelastic nanobeam with two temperatures subjected to ramp-type heating, revealing insights into the behavior of nanobeam structures under the influence of magneto-electro-piezo-thermoelastic effects during ramp-type heating scenarios.

Piezoelectric materials are widely employed in diverse real-world applications, yet their behavior at the free surface of the hygro-thermo-piezo-elastic medium remains inadequately understood. The objective of this study is to develop an innovative mathematical model to analyze the behavior of plane waves in piezo-thermoelastic materials. Additionally, the study aims to investigate the influence of moisture and temperature diffusivities, as well as moisture content, on the distribution of physical properties within the thermo-piezo-elasticmaterial. This study provides a deeper understanding of these materials' behavior, aiding in optimizing their design for practical applications.

2 Fundamental Equations of Hygro-thermo-piezo-elastic Medium

Following Yadav et al. [40], Barak and Gupta [41], Szekeres [42, 43], and Hosseini and Ghadiri [44],the total moisture flux f_i and heat flux q_i and the basic relationship for a coupled anisotropic hygro-thermo-piezo-elasticmedium are:

$$q_i = -D_{ij}^T T_{,i} - q_{ij}^m m_{,i}, \tag{1}$$

$$f_i = -D_{ij}^m m_{,i} - Q_{ij}^T T_{,i}. \tag{2}$$

The hygro-piezoelectric medium facilitates the transmission of elastic, moisture, electro-magnetic, and thermal waves. The constitutive equations pertaining to this medium are stated in the following manner:

$$D_i = \eta_{ijk} e_{jk} + \varepsilon_{ij} E_j + \tau_i T + d_i m, E_i = -\phi_{,i} \tag{3}$$

$$\rho T_0 \dot{S} = -q_{i,i}, \; \rho T_0 S = \frac{\beta_{ij}^T T_0}{\rho C_E} e_{kk} + T - T_0 \tau_i \phi_{,i}, \tag{4}$$

$$-q_{i,i} = D_{ij}^T T_{,ii} + q_{ij}^m m_{,ii}, \tag{5}$$

$$\left. \begin{array}{l} \dot{J} = -f_{i,i}, \\ J = m + \frac{\beta_{ij}^m D_{ij}^m m_0}{K_m} e_{kk} - m_0 d_i \phi_{,i} \end{array} \right\}, \tag{6}$$

$$-f_{i,i} = D_{ij}^m m_{,ii} + Q_{ij}^T T_{,ii}, \tag{7}$$

$$\sigma_{ij} = c_{ijkl} e_{kl} - \eta_{ijk} E_k + \beta_{ij}^T T + \beta_{ij}^m m, \tag{8}$$

$$\left. \begin{array}{l} \sigma_{11} = c_{11} u_{1,1} + c_{12} u_{2,2} + c_{13} u_{3,3} - \beta_1^T T - \beta_1^m m + \eta_{31\}} \phi_{,3}, \\ \sigma_{12} = c_{66} \left(u_{1,2} + u_{2,1} \right), \\ \sigma_{13} = c_{55} \left(u_{1,3} + u_{3,1} \right) + \eta_{15} \phi_{,1}, \\ \sigma_{22} = c_{12} u_{1,1} + c_{22} u_{2,2} + c_{23} u_{3,3} - \beta_2^T T - \beta_2^m m + \eta_{32\}} \phi_{,3}, \\ \sigma_{23} = c_{44} \left(u_{2,3} + u_{3,2} \right) + \eta_{24} \phi_{,2}, \\ \sigma_{33} = c_{13} u_{1,1} + c_{23} u_{2,2} + c_{33} u_{3,3} - \beta_3^T T - \beta_3^m m + \eta_{33\}} \phi_{,3}, \end{array} \right\} \tag{9}$$

$$\left. \begin{array}{l} D_1 = \eta_{15} \left(u_{1,3} + u_{3,1} \right) - \varepsilon_{11} \phi_{,1}, \\ D_2 = \eta_{24} \left(u_{2,3} + u_{3,2} \right) - \varepsilon_{22} \phi_{,2} \\ D_3 = \eta_{31} u_{1,1} + \eta_{32} u_{2,2} + \eta_{33} u_{3,3} - \varepsilon_{33} \phi_{,3} + \tau_3 T + d_3 m. \end{array} \right\} \tag{10}$$

Equation of motion:

$$\sigma_{ji,j} = \rho \ddot{u}_i. \tag{11}$$

The following is the outcome of Eqs. (1), (4), and (5):

$$D_i^T T_{,ii} + q_i^m m_{,ii} - \dot{T} - \frac{\beta_i^T T_0}{\rho C_E} \dot{u}_{j,j} + T_0 \tau_i \dot{\phi}_{,i} = 0. \tag{12}$$

The following is the outcome of Eqs. (2), (6), and (7):

$$D_i^m m_{,ii} + Q_i^T T_{,ii} - \dot{m} - \frac{\beta_i^m D_i^m m_0}{K_m} \dot{u}_{j,j} + m_0 d_i \dot{\phi}_{,i} = 0. \tag{13}$$

Equation (3) may be written as follows:

$$D_{i,i} = 0 \; \Rightarrow \; D_{1,1} + D_{2,2} + D_{3,3} = 0, \tag{14}$$

where, $\beta_{ij}^T = \beta_i^T \delta_{ij}$, $\beta_{ij}^m = \beta_i^m \delta_{ij}$, $D_{ij}^T = D_i^T \delta_{ij}$, $D_{ij}^m = D_i^m \delta_{ij}$, $q_{ij}^m = q_i^m \delta_{ij}$, $Q_{ij}^T = Q_i^T \delta_{ij}$, and, i, j is not summed.

3 Modeling of the Problem

We assume a homogeneous orthotropic hygro-thermo-piezo-elastic half-space, and we adopt a Cartesian coordinate system (x, y, z). The half-space is characterized by uniform initial temperature T_0 and moisture m_0, as shown in Fig. 1. The propagation of hygro-thermal-elastic waves occurs within the xz plane, with all physical field variables function of t, x, and z.

The set of Eqs. (9)–(14) represents the governing equation that can be mathematically described in the $xz-$ plane as:

$$c_{11}\frac{\partial^2 u}{\partial x^2} + c_{55}\frac{\partial^2 u}{\partial z^2} + (c_{13} + c_{55})\frac{\partial^2 w}{\partial x \partial z} + (\eta_{31} + \eta_{15})\frac{\partial^2 \phi}{\partial x \partial z} - \beta_1^T\frac{\partial T}{\partial x} - \beta_1^m\frac{\partial m}{\partial x} = \rho\ddot{u},$$
(15)

$$(c_{13} + c_{55})\frac{\partial^2 u}{\partial x \partial z} + c_{55}\frac{\partial^2 w}{\partial x^2} + c_{33}\frac{\partial^2 w}{\partial z^2} + \eta_{15}\frac{\partial^2 \phi}{\partial x^2} + \eta_{33}\frac{\partial^2 \phi}{\partial z^2} - \beta_3^T\frac{\partial T}{\partial z} - \beta_3^m\frac{\partial m}{\partial z} = \rho\ddot{w},$$
(16)

$$D_1^T\frac{\partial^2 T}{\partial x^2} + D_3^T\frac{\partial^2 T}{\partial z^2} + q_1^m\frac{\partial^2 m}{\partial x^2} + q_3^m\frac{\partial^2 m}{\partial z^2} - \frac{\partial T}{\partial t} - \frac{T_0}{\rho C_E}\left(\beta_1^T\frac{\partial^2 u}{\partial x \partial t} + \beta_3^T\frac{\partial^2 w}{\partial z \partial t}\right) + T_0\tau_3\frac{\partial^2 \phi}{\partial z \partial t} = 0,$$
(17)

$$Q_1^T\frac{\partial^2 T}{\partial x^2} + Q_3^T\frac{\partial^2 T}{\partial z^2} + D_1^m\frac{\partial^2 m}{\partial x^2} + D_3^m\frac{\partial^2 m}{\partial z^2} - \frac{\partial m}{\partial t} - \frac{m_0}{K_m}\left(\beta_1^T D_1^m\frac{\partial^2 u}{\partial x \partial t} + \beta_3^T D_3^m\frac{\partial^2 w}{\partial z \partial t}\right) + m_0 d_3\frac{\partial^2 \phi}{\partial z \partial t} = 0,$$
(18)

$$(\eta_{15} + \eta_{31})\frac{\partial^2 u}{\partial x \partial z} + \eta_{15}\frac{\partial^2 w}{\partial x^2} + \eta_{33}\frac{\partial^2 w}{\partial z^2} - \varepsilon_{11}\frac{\partial^2 \phi}{\partial x^2} - \varepsilon_{33}\frac{\partial^2 \phi}{\partial z^2} + \tau_3\frac{\partial T}{\partial z} + d_3\frac{\partial m}{\partial z} = 0,$$
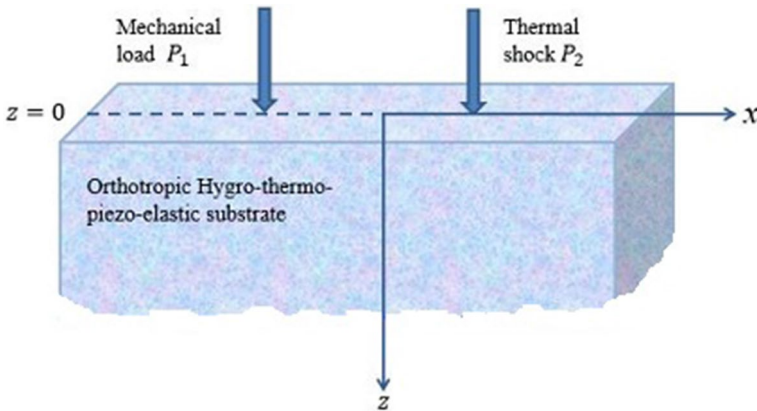(19)

Fig. 1 Schematic representation of the problem

where, $\vec{u} = (u, 0, w)$, $\beta_1^T = (c_{11} + c_{13})\alpha_{11}^T + c_{13}\alpha_{11}^T$, $\beta_3^T = 2c_{13}\alpha_{33}^T + c_{33}\alpha_{33}^T$,
$\beta_1^m = (c_{11} + c_{13})\alpha_{11}^m + c_{13}\alpha_{11}^m$, $\beta_3^m = 2c_{13}\alpha_{33}^m + c_{33}\alpha_{33}^m$, the constants α_{11}^m, α_{33}^m for the moisture expansion and α_{11}^T, α_{33}^T for the linear thermal expansion.

4 Solution of the Problem

The technique of normal mode analysis has broad applications across several disciplines. It enables the calculation of solutions without imposing preconceptions on the studied variables, such as horizontal and vertical displacements, electric potential, temperature, and moisture. For the normal mode approach, the solution for these variables can be broken down as follows [45]:

$$(u, w, \phi, T, m)(x, z, t) = (u', w', \phi', T', m')(z) \exp[ik(x - ct)], \qquad (20)$$

where,$\omega = kc$ be the frequency,k be the wave number in the $x-$ direction and u', w', $\phi' T'$, and m' are the function of z only,

Equations (15) through (19) and Eq. (20) together produce a homogeneous set of equations in five unknowns u', w', ϕ', T', m' as

$$\Omega R = 0 \qquad (21)$$

where, $\Omega = \begin{bmatrix} a_{11} + c_{55}D^2 & -a_{12}D & -a_{13}D & a_{14} & a_{15} \\ a_{21}D & a_{22} - c_{33}D^2 & a_{23} - \eta_{33}D^2 & \beta_3^T D & \beta_3^m D \\ a_{31} & a_{32}D & -a_{33}D & a_{34} - D_1^T D^2 & a_{35} - q_1^m D^2 \\ a_{41} & a_{42}D & -a_{43}D & a_{44} - Q_3^T D^2 & a_{45} - D_3^m D^2 \\ a_{51}D & a_{52} - \eta_{33}D^2 & \varepsilon_{33}D^2 - a_{53} & -\tau_3 D & -d_3 D \end{bmatrix}$,

$R = \begin{bmatrix} u' \\ w' \\ \phi' \\ T' \\ m' \end{bmatrix}$, and $a_{11} = \rho\omega^2 - c_{11}k^2$, $a_{12} = -(c_{13} + c_{55})\imath k$, $a_{13} = -(\eta_{31} + \eta_{15})\imath k$,

$a_{14} = -\beta_1^T \imath k$, $a_{15} = -\beta_1^m \imath k$, $a_{21} = -(c_{13} + c_{55})\imath k$, $a_{22} = c_{55}k^2 - \rho\omega^2$, $a_{23} = \eta_{15}k^2$,
$a_{31} = -\frac{T_0\beta_1^T k\omega}{\rho C_e}$, $a_{32} = \frac{T_0\beta_3^T \imath\omega}{\rho C_e}$, $a_{33} = T_0\tau_3 \imath\omega$, $a_{34} = k^2 D_1^T + \imath\omega$, $a_{35} = k^2 q_1^m$,
$a_{41} = -\frac{m_0\beta_1^T D_1^m k\omega}{K_m}$, $a_{42} = \frac{m_0\beta_3^T D_3^m \imath\omega}{K_m}$, $a_{43} = m_0 d_3 \imath\omega$, $a_{44} = Q_1^T k^2$, $a_{41} = \frac{m_0\beta_1^T D_1^m k\omega}{K_m}$,
$a_{51} = -(\eta_{15} + \eta_{31})\imath k$, $a_{52} = \eta_{15}k^2$, $a_{53} = \varepsilon_{11}k^2 D = \partial/\partial z$.

The characteristic equation is obtained by nullifying the determinant of the matrix presented in Eq. (21) to find a non-trivial solution.

$$(B_0 D^{10} + B_1 D^8 + B_2 D^6 + B_3 D^4 + B_4 D^2 + B_5)\{\phi'(z), T'(z), u'(z), w'(z), m'(z)\} = 0 \qquad (22)$$

the coefficients B_i, $i = 1 - 5$ are provided in the Appendix.

The factorization of Eq. (22) may be expressed as.

$$\prod_{j=1}^{5} \left(D^2 - \lambda_j^2 \right) \{ \phi'(z),\, T'(z),\, u'(z),\, w'(z),\, m'(z) \} = 0.$$ (23)

The solutions of Eq. (23) are bounded as $z \to \infty$ and given as follows:

$$\left(u',\, w',\, \phi',\, T',\, m' \right) = \sum_{n=1}^{5} \left(M_n,\, L_{1n}M_n,\, L_{2n}M_n,\, L_{3n}M_n,\, L_{4n}M_n \right) \exp\left(-\lambda_n z \right),$$ (24)

$$
\begin{bmatrix} L_{1n} \\ L_{2n} \\ L_{3n} \\ L_{4n} \end{bmatrix} =
\begin{bmatrix}
a_{12}\lambda_n & a_{13}\lambda_n & a_{14} & a_{15} \\
a_{22} - c_{33}\lambda_n^2 & a_{23} - \eta_{33}\lambda_n^2 & -\beta_3^T\lambda_n & -\beta_3^m\lambda_n \\
a_{32}\lambda_n & -a_{33}\lambda_n & -a_{34} + D_3^T\lambda_n^2 & -a_{35} + q_3^m\lambda_n^2 \\
a_{42}\lambda_n & -a_{43}\lambda_n & -a_{44} + Q_3^T\lambda_n^2 & -a_{45} + D_3^m\lambda_n^2
\end{bmatrix}^{-1}
\begin{bmatrix} -a_{11} - c_{55}\lambda_n^2 \\ \lambda_n a_{21} \\ a_{31} \\ a_{41} \end{bmatrix},
$$

and λ_n^2, $(n = 1 - 5)$ are the solutions of the characteristics Eq. (23).

By using Eq. (24) in Eqs. (9)-(10) in the xz plane and applying the normal mode approach yields the subsequent outcomes:

$$\left(\sigma_{xx},\, \sigma_{zz},\, \sigma_{xz},\, D_x,\, D_z \right) = \sum_{n=1}^{5} \left(L_{5n},\, L_{6n},\, L_{7n},\, L_{8n},\, L_{9n} \right) \exp(-\lambda_n x_3).$$ (25)

5 Boundary Conditions

The free surface $(z = 0)$ of the considered model is subjected to mechanical load and thermal shock. Following Dutta et al. [46], the subsequent boundary conditions aid in solving the governing equations within a half-space domain $(x, y, z \geq 0)$.

Mechanical boundary conditions:

$$\sigma_{zz}(x, 0, t) = P_1(x, t) = -P_1^* \exp\{ \imath k(x - ct) \},\, \sigma_{xz}(x, 0, t) = 0$$ (26)

Thermal boundary condition:

$$T(x, 0, t) = P_2(x, t) = P_2^* \exp\{ \imath k(x - ct) \},$$ (27)

where, $P_1(x, t)$ and $P_2(x, t)$ indicated the arbitrary functions of (x, t), P_1^*, P_2^* are constant.

Electrical boundary condition:

$$\phi_{,z}(x, 0, t) = 0.$$ (28)

Electrical displacement boundary condition:

$$D_{,z}(x, 0, t) = 0.$$ (29)

Upon substitution of the postulated solutions into the prescribed boundary conditions (26)–(29), the coefficients $M_n (n = 1 - 5)$, yield

$$\sum_{n=1}^{5} L_{6n} M_n = -P_1^*, \tag{30}$$

$$\sum_{n=1}^{5} L_{7n} M_n = 0, \tag{31}$$

$$\sum_{n=1}^{5} L_{3n} M_n = P_2^*, \tag{32}$$

$$\sum_{n=1}^{5} \lambda_n L_{2n} M_n = 0, \tag{33}$$

$$\sum_{n=1}^{5} \lambda_n L_{9n} M_n = 0, \tag{34}$$

where, $L_{5n} = c_{11} \imath k - c_{13} \lambda_n L_{1n} - \eta_{31} \lambda_n L_{2n} - \beta_1^T L_{3n} - \beta_1^m L_{4n}$, $L_{7n} = -c_{55} (\lambda_n - \imath k L_{1n}) + \eta_{15} \imath k L_{2n}$.

$L_{6n} = c_{13} \imath k - c_{33} \lambda_n L_{1n} - \eta_{33} \lambda_n L_{2n} - \beta_3^T L_{3n} - \beta_3^m L_{4n}$,
$L_{8n} = -\eta_{15} (\lambda_n - \imath k L_{1n}) - \varepsilon_{11} \imath k L_{2n}$.

$L_{9n} = \eta_{31} \imath k - \eta_{33} \lambda_n L_{1n} + \varepsilon_{33} \lambda_n L_{2n} + \tau_3 L_{3n} + d_3 L_{4n}$.

To obtain the value of $M_n (n = 1 - 5)$, the Eqs. (30) to (34) can be solved using the inverse matrix method, which can be carried out as follows:

$$\begin{bmatrix} M_1 \\ M_2 \\ M_3 \\ M_4 \\ M_5 \end{bmatrix} = \begin{bmatrix} L_{61} & L_{62} & L_{63} & L_{64} & L_{65} \\ L_{71} & L_{72} & L_{73} & L_{74} & L_{75} \\ L_{31} & L_{32} & L_{33} & L_{34} & L_{35} \\ \lambda_1 L_{21} & \lambda_2 L_{22} & \lambda_3 L_{23} & \lambda_4 L_{24} & \lambda_5 L_{25} \\ \lambda_1 L_{91} & \lambda_2 L_{92} & \lambda_3 L_{93} & \lambda_4 L_{94} & \lambda_5 L_{95} \end{bmatrix}^{-1} \begin{bmatrix} -P_1^* \\ 0 \\ P_2^* \\ 0 \\ 0 \end{bmatrix} \tag{35}$$

This approach enables the derivation of precise analytical expressions for the diverse components of the displacement vector, electric displacement, stresses, temperature, and electric potential.

6 Validation

Considering isotropy and neglecting piezo and pyro-electric effects, we have

$c_{11} = \lambda + 2\mu$, $c_{33} = \lambda + 2\mu$, $c_{13} = \lambda$, $c_{55} = \mu$, $\beta_1^T = \beta_3^T = \beta^T$, $\beta_1^m = \beta_3^m = \beta^m$, $D_1^T = D_3^T = D^T$, $D_1^m = D_3^m = D^m$, $q_1^m = q_3^m = D_T^m$, $Q_1^T = Q_3^T = D_m^T$, $d_3 = 0$, $\tau_3 = 0$,

$\varepsilon_{11} = \varepsilon_{33} = 0$, $\eta_{31} = \eta_{33} = \eta_{15} = 0$, the above model transforms into a thermo-hygro-elastic model as developed by Yadav et al. [40].

The fundamental Eqs. (15) to (19) regulating the system may be simplified as

$$(\lambda + 2\mu)\frac{\partial^2 u}{\partial x^2} + \mu\frac{\partial^2 u}{\partial z^2} + ((\lambda + \mu))\frac{\partial^2 w}{\partial x \partial z} + -\beta^T\frac{\partial T}{\partial x} - \beta^m\frac{\partial m}{\partial x} = \rho\ddot{u}, \qquad (36)$$

$$(\lambda + \mu)\frac{\partial^2 u}{\partial x \partial z} + \mu\frac{\partial^2 w}{\partial x^2} + (\lambda + 2\mu)\frac{\partial^2 w}{\partial z^2} + -\beta^T\frac{\partial T}{\partial z} - \beta^m\frac{\partial m}{\partial z} = \rho\ddot{w}, \qquad (37)$$

$$D^T\left(\frac{\partial^2 T}{\partial x^2} + \frac{\partial^2 T}{\partial z^2}\right) + D_T^m\left(\frac{\partial^2 m}{\partial x^2} + \frac{\partial^2 m}{\partial z^2}\right) - \frac{\partial T}{\partial t} - \frac{\beta^T T_0}{\rho C_E}\left(\frac{\partial^2 u}{\partial x \partial t} + \frac{\partial^2 w}{\partial z \partial t}\right) = 0, \qquad (38)$$

$$D_m^T\left(\frac{\partial^2 T}{\partial x^2} + \frac{\partial^2 T}{\partial z^2}\right) + D^m\left(\frac{\partial^2 m}{\partial x^2} + \frac{\partial^2 m}{\partial z^2}\right) - \frac{\partial m}{\partial t} - \frac{\beta^m m_0 D^m}{K_m}\left(\frac{\partial^2 u}{\partial x \partial t} + \frac{\partial^2 w}{\partial z \partial t}\right) = 0. \qquad (39)$$

7 Numerical Results and Discussion

A numerical experiment has been conducted using MATLAB software to investigate the impact of hygrothermal conditions on the physical distribution of piezo-thermoelastic material. The values for hygro parameters and material constants for cadmium selenide, as presented in Table 1, are adopted based on the works of Yadav et al.[47].

Table 1 Values of the materials constants

Symbol	Value	Symbol	Value
c_{11}	$74.1 \times 10^9\,\mathrm{Nm^{-2}}$	ε_{11}	$8.26 \times 10^{-11}\,\mathrm{C^2\,N^{-1}\,m^{-2}}$
c_{12}	$45.2 \times 10^9\,\mathrm{Nm^{-2}}$	ε_{33}	$9.03 \times 10^{-11}\,\mathrm{C^2\,N^{-1}\,m^{-2}}$
c_{13}	$39.3 \times 10^9\,\mathrm{Nm^{-2}}$	τ_3	$-2.9 \times 10^{-6}\,\mathrm{cm^{-2}\,K^{-1}}$
c_{33}	$83.6 \times 10^9\,\mathrm{Nm^{-2}}$	T_0	$298\,\mathrm{K}$
c_{55}	$13.2 \times 10^9\,\mathrm{Nm^{-2}}$	C_E	$260\,\mathrm{J\,kg^{-1}\,K^{-1}}$
β_1^T	$6.21 \times 10^5\,\mathrm{Nm^{-2}\,K^{-1}}$	ρ	$5504\,\mathrm{kg\,m^{-3}}$
β_3^T	$5.51 \times 10^5\,\mathrm{Nm^{-2}\,K^{-1}}$	η_{31}	$-0.160\,\mathrm{cm^{-2}}$
m_0	$10\,\%$	η_{15}	$-0.138\,\mathrm{cm^{-2}}$
D_1^m	$0.8 \times 10^{-4}\,\mathrm{m^2\,s^{-1}}$	D_1^T	$50 \times 10^{-4}\,\mathrm{m^2\,s^{-1}}$
D_3^m	$1.1 \times 10^{-4}\,\mathrm{m^2\,s^{-1}}$	D_3^T	$75 \times 10^{-4}\,\mathrm{m^2\,s^{-1}}$
η_{33}	$0.347\,\mathrm{cm^{-2}}$	ω	$100\,\mathrm{Hz}$
q_1^m	$18.5 \times 10^{-5}\,\mathrm{m^2(^0K)/s(\%H_2O)}$	Q_1^T	$31.3 \times 10^{-6}\,\mathrm{m^2(\%H_2O)/s(^0K)}$
q_3^m	$18 \times 10^{-5}\,\mathrm{m^2(^0K)/s(\%H_2O)}$	Q_3^T	$33.3 \times 10^{-6}\,\mathrm{m^2(\%H_2O)/s(^0K)}$
K_m	$2.2 \times 10^{-8}\,\mathrm{kg/msM}$	d_3	$0.34\,\mathrm{cm^{-2}\,K^{-1}}$

During the numerical method outlined previously, we focus on the real components of the stress tensor $\left(\sigma_{xx}, \sigma_{zz}, \sigma_{xz}\right)$, electric displacement $\left(D_x, D_z\right)$, displacement vector (u, w), temperature T, and electric potential ϕ. We calculated and plotted the physical distribution of these components by varying moisture concentrations, moisture diffusivity, and temperature diffusivity for fixed $\beta_1^m = 0.8 \times 10^{-4}$, $\beta_3^m = 1.1 \times 10^{-4}$. The sub-figures of the resulting graph present overlapping curves to clearly illustrate any subtle differences, thereby aiding in comprehending intricate details at a micro-scale.

The first category, Fig. 2a–i depicted the effect of various levels of moisture concentration $\left(m_0 = 10\%, 20\%, 30\%, 40\%\right)$ on the hygro-piezo-thermal-elastic-electric wave propagation with the distance z. All calculations have been evaluated with time $t = 1.5$ and assumed constants $P_1^* = 0.01$ and $P_1^* = 0.02$. The sky blue, orange, yellow, and purple linesrelated to the moisture concentration $m_0 = 10\%, 20\%, 30\%, 40\%$, respectively.

The distribution of displacement expresses the elastic wave. Within the given range $0 \le z \le 0.5$, the horizontal displacement component u exponentially decreases from a negative value to its minimum value. As shown in Fig. 2a, with a further increase of z, the horizontal displacement progressively increases and tends towards zero. The vertical displacement component w starts with a positive value at the maximum point and decreases exponentially, converging to zero as z approaches infinity, as illustrated in Fig. 2b. The horizontal displacement component's distribution is directly proportional to the concentration of the moisture, whereas the vertical displacement component's distribution is inversely proportional to it.

The potential distribution field ϕ represents the electric wave, starting from its minimum negative point and sharply increasing as z increases, ultimately vanishing as z approaches infinity, as illustrated in Fig. 2c. The thermal temperature T represents the thermal wave, decreasing exponentially within the range $0 \le z \le 0.05$. Subsequently, with a further increment of z the u gradually increases and approaches zero, as shown in Fig. 2d. The amount of electric potential and temperature distributions is inversely proportional to the moisture concentration, with higher moisture concentrations resulting in lower amounts of both distributions.

The mechanical wave generated by the stress components is shown in Fig. 2e–g. Figure 2e illustrates the distribution profile of the stress component σ_{xx}, which starts from a maximum value and decreases exponentially, approaching zero as z tends to infinity. Figure 2f reveals that the stress component σ_{zz} distribution starts from zero, increases exponentially within the range $0 \le z \le 0.3$, and then tends to zero as z further increases. Figure 2g demonstrates that the distribution profile of the stress component σ_{xz} follows a pattern almost identical to that of the stress component σ_{zz}. The σ_{xz} distribution curve starts from zero, satisfying the boundary condition (26), i.e., $\sigma_{xz}(x, 0, t) = 0$. The noted observation enhances assurance in the accuracy and reliability of our numerical coding, indicating the accurate implementation of the boundary condition (36). Figure 2e–g distinctly illustrate the considerable influence of moisture content on the mechanical wave.

The electrical displacement D_x and D_z are shown in Fig. 2h, i. The amplitude of D_x start from a positive value at the maximum point and reaches minima its negative value with a slight increase of z. Further increase of z the amplitude increases and
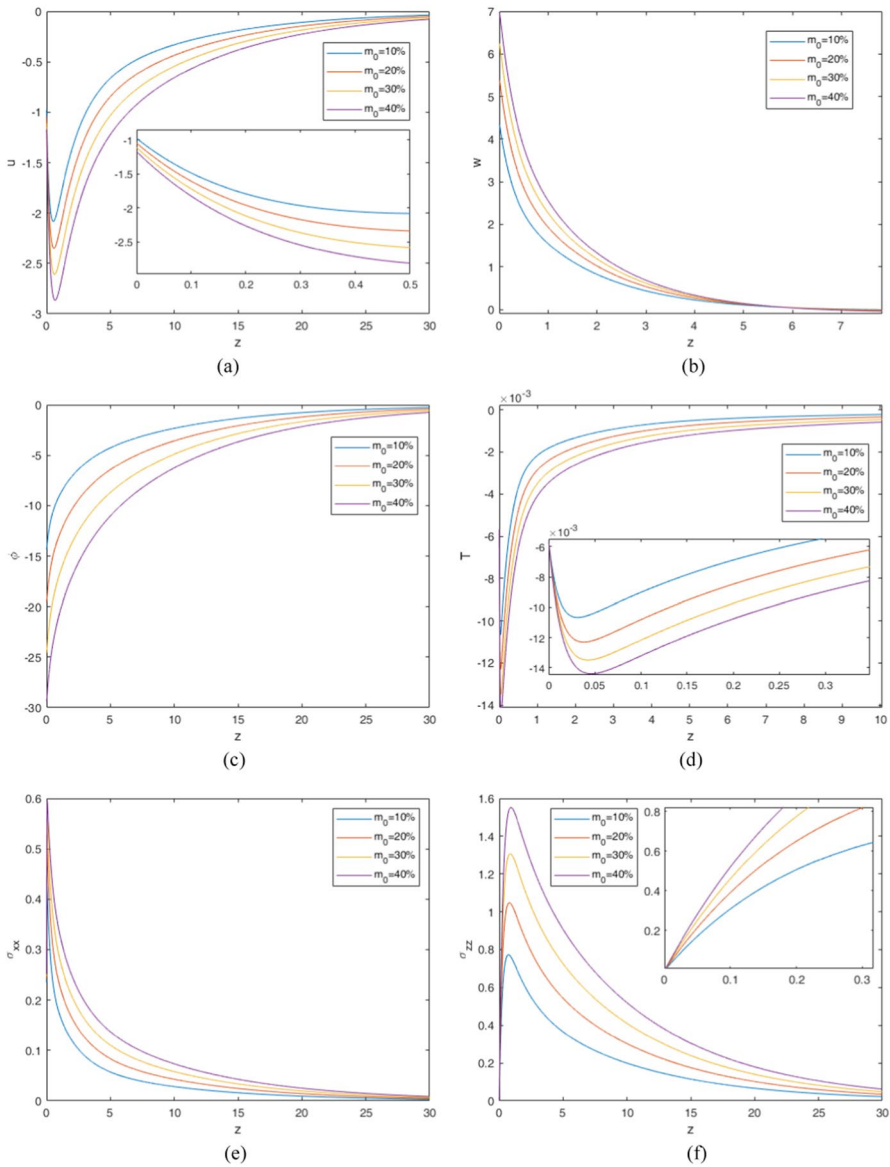
Fig. 2 a–i Distribution of the physical quantities with respect to z for various values of moisture concentration $m_0 = 10\%$, 20%, 30%, 40%, at $D_1^m = 0.8 \times 10^{-4}$, $D_3^m = 1.1 \times 10^{-4}$, $D_1^T = 50 \times 10^{-4}$, $D_1^T = 75 \times 10^{-4}$

reaches to zero. The amplitude of the D_z start from positive value at the maximum point decreases exponentially and tends to zero with z. Figure 2h, i suggest that the electrical displacement increases with the increase of moisture concentration.

The second category, Fig. 3a–i shows the effect of moisture diffusivity param-

eters $\left(D_1^m = 0.8 \times 10^{-4}, D_3^m = 1.1 \times 10^{-4}\right)$, $\left(D_1^m = 0.8 \times 10^{-3}, D_3^m = 1.1 \times 10^{-3}\right)$,

(g)

(h)

(i)
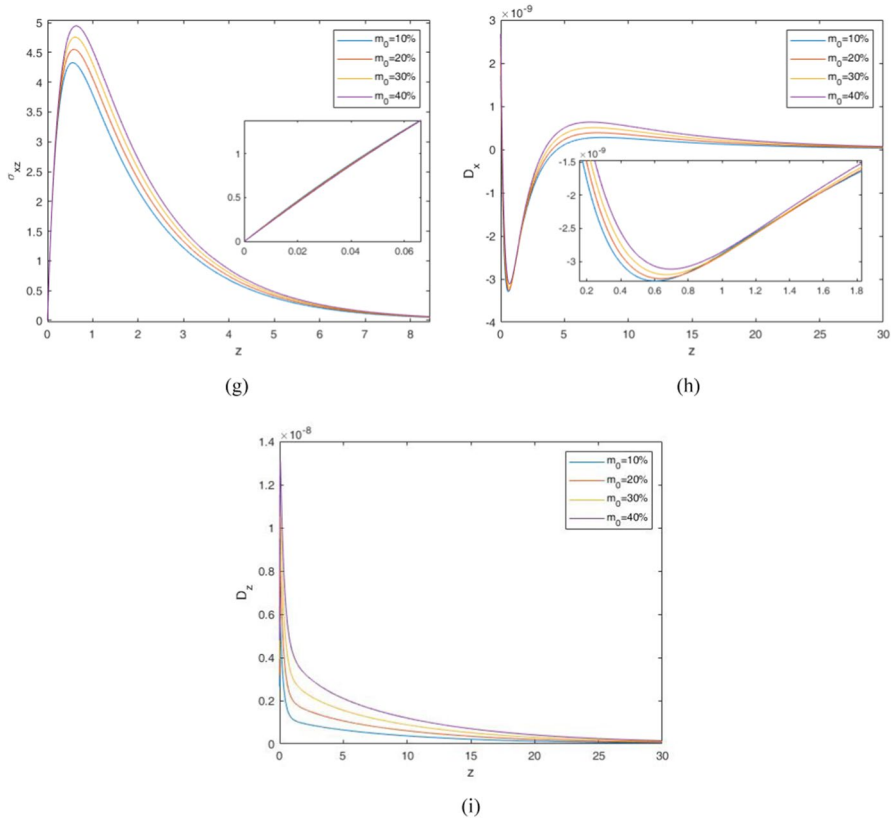
Fig. 2 (continued)

$\left(D_1^m = 0.8 \times 10^{-2}, D_3^m = 1.1 \times 10^{-2} \right)$, $\left(D_1^m = 0.8 \times 10^{-1}, D_3^m = 1.1 \times 10^{-1} \right)$ on the profiles of the hygro-piezo-thermo-elastic model with a fixed time $t = 1.5$ and assumed constant $P_1^* = 0.01$ and $P_1^* = 0.02$. From these figures, note that all physical field distributions exhibit similar behavior, as described in Fig. 2a–i.

The significant impact of moisture diffusivity observes a fascinating complexity that defies a simplistic direct or inverse proportionality with moisture diffusivity. Rather than adhering to predictable patterns, the relationship between moisture diffusivity and the distribution profiles unfolds in a nuanced manner, showcasing the richness of interactions at play. It becomes apparent that the impact of moisture diffusivity is not uniform, leading to intricate variations in the distribution profiles. This departure from conventional expectations adds a layer of sophistication to the understanding of the system. To enhance clarity, we employ descriptive language to highlight specific instances where the influence of moisture diffusivity manifests in unexpected ways. By navigating through these specific scenarios or depth ranges,
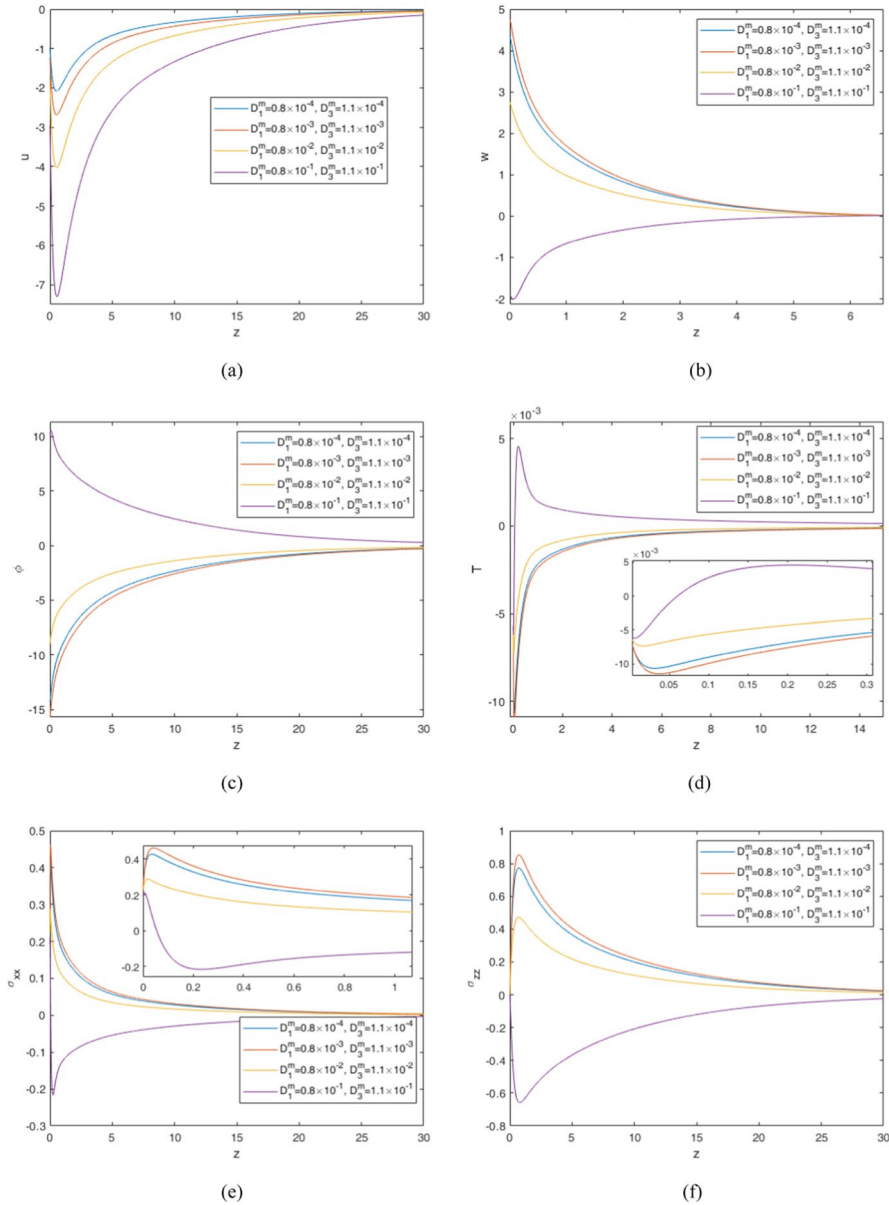
Fig. 3 **a–i** Distribution of the physical quantities with respect to z for various values of moisture diffusivity $D_1^m = 0.8 \times 10^{-4}$, $D_3^T = 1.1 \times 10^{-4}$, $D_1^m = 0.8 \times 10^{-3}$, $D_3^m = 1.1 \times 10^{-3}$, $D_1^m = 0.8 \times 10^{-2}$, $D_3^m = 1.1 \times 10^{-2}$, $D_1^m = 0.8 \times 10^{-1}$, $D_3^m = 1.1 \times 10^{-1}$, at $m_0 = 10\%$, $D_1^T = 50 \times 10^{-4}$, $D_3^T = 75 \times 10^{-4}$

the graphical discussion unveils a tapestry of complexities, offering a more profound and convincing interpretation of the observed phenomena.

In essence, this approach acknowledges the intricate and non-linear nature of the relationship between moisture diffusivity and physical distribution profiles and

(g)

(h)

(i)
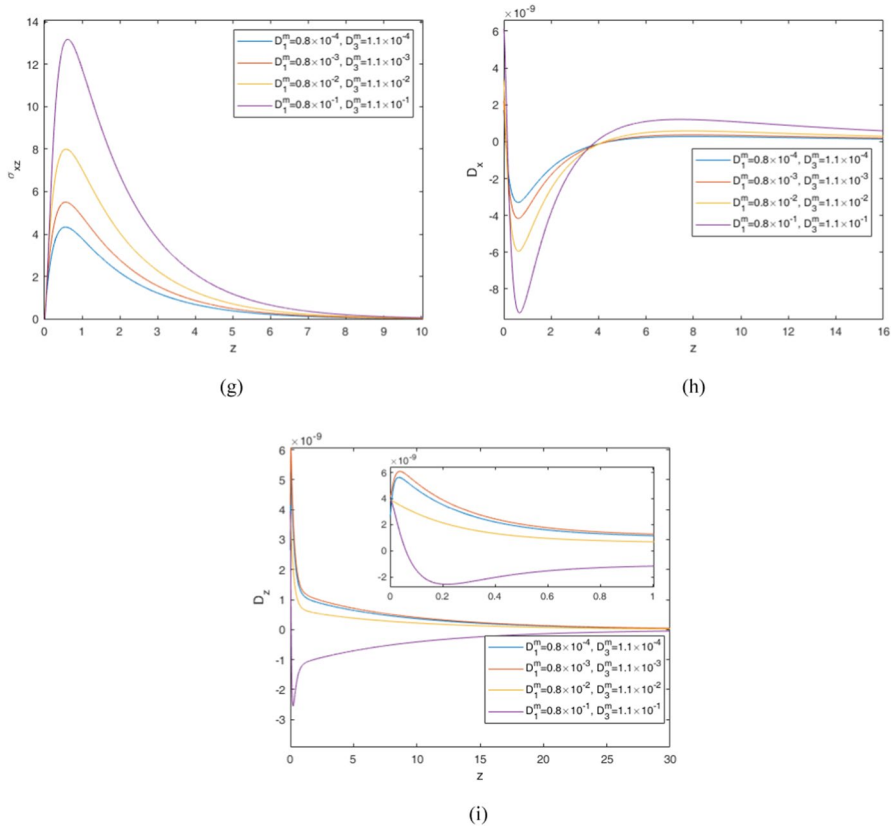
Fig. 3 (continued)

persuasively underscores the need to embrace the complexity inherent in the system under investigation. The physical properties of the hygro-piezo-thermo-elastic model always tend to the equilibrium state as z approaches infinity.

The third category, Fig. 4a–i shows the effect of temperature diffusivity parameters $\left(D_1^T = 50 \times 10^{-4}, \quad D_3^T = 75 \times 10^{-4}\right)$, $\left(D_1^T = 50 \times 10^{-3}, \quad D_3^T = 75 \times 10^{-3}\right)$, $\left(D_1^T = 50 \times 10^{-2}, D_3^T = 75 \times 10^{-2}\right)$, $\left(D_1^T = 50 \times 10^{-1}, D_3^T = 75 \times 10^{-1}\right)$ on the various distribution profiles of the hygro-piezo-thermo-elastic model with a fixed time $t = 1.5$ and assumed constant $P_1^* = 0.01$ and $P_1^* = 0.02$. Upon examination of these figures, it becomes apparent that all of the field distributions exhibit a similar trend, as depicted in Fig. 2a–i. Notably, the impact of temperature diffusivity is prominently manifested in the aforementioned figures. It should also be pointed out that the physical properties of the hygro-piezo-thermo-elastic model invariably tend towards an equilibrium state as z approaches infinity.

The initial three categories illustrate the physical field distribution at a fixed value of $x = 0.1$ across various profiles. Conversely, the fourth category, presented in Fig. 5a–i, showcases 3D plots of the solutions in the xz plane at a fixed time $t = 1.5$,
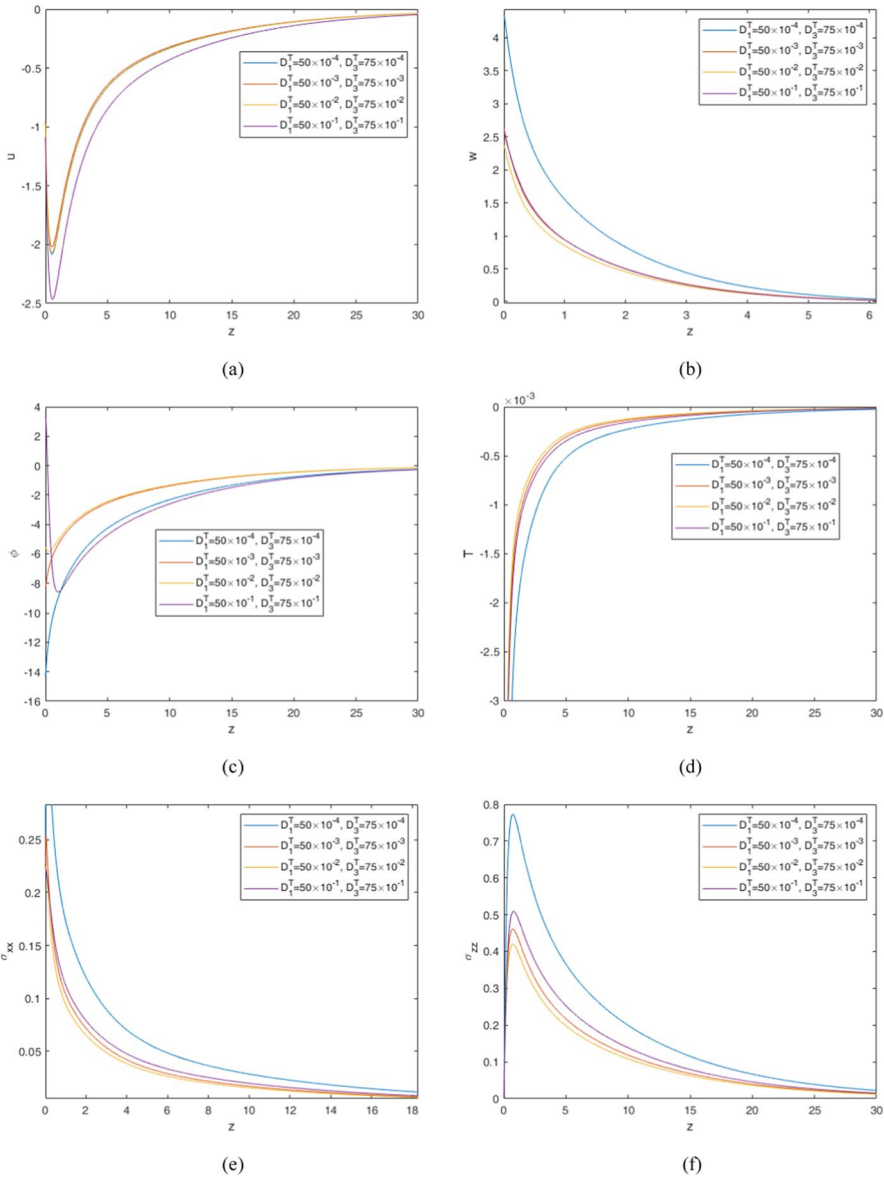
Fig. 4 **a–i** Distribution of the physical quantities with respect to z for various values of temperature diffusivity $D_1^T = 50 \times 10^{-4}$, $D_3^T = 75 \times 10^{-4}$, $D_1^T = 50 \times 10^{-3}$, $D_3^T = 75 \times 10^{-3}$, $D_1^T = 50 \times 10^{-2}$, $D_3^T = 75 \times 10^{-2}$, $D_1^T = 50 \times 10^{-1}$, $D_3^T = 75 \times 10^{-1}$, at $m_0 = 10\,\%$, $D_1^m = 0.8 \times 10^{-4}$, $D_3^T = 1.1 \times 10^{-4}$

allowing an exploration of the influence of x on the distribution patterns. All figures were generated within the range of $-10 \leq x \leq 10$ and $0 \leq z \leq 30$. The observation from Fig. 5a–i are as follows:
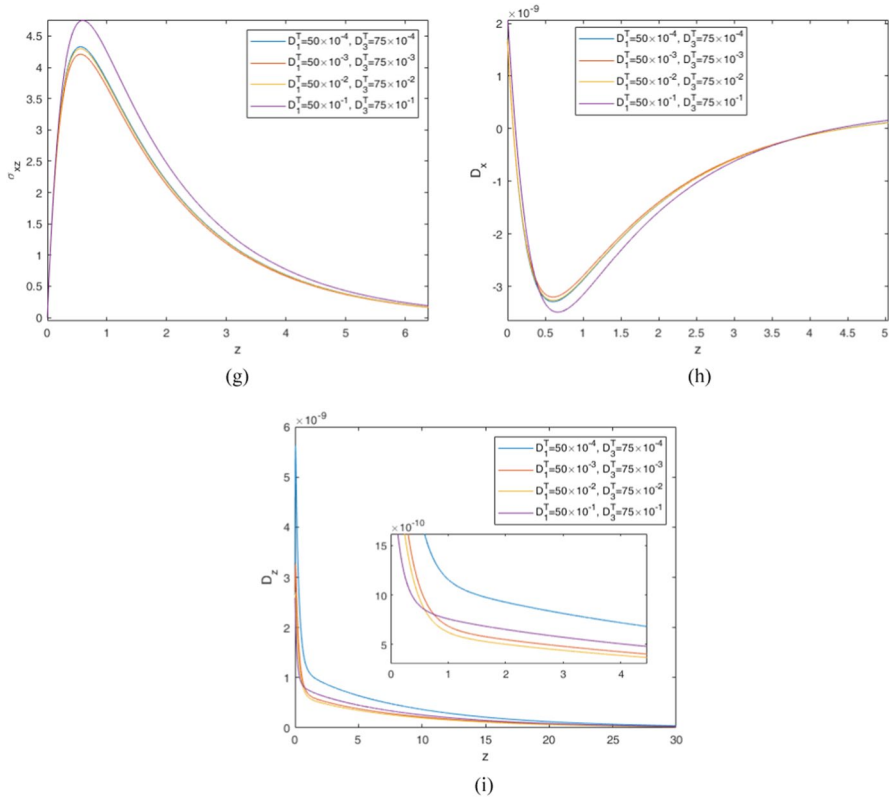
(g)   (h)

(i)

Fig. 4 (continued)

- Across the entire range of x, all function profiles display a nearly uniform distribution characterized by alternating peaks.
- The green color region signifies displacement values approaching zero, affirming the theoretical assumption of boundedness in the solution as $z \rightarrow \infty$.
- By inspecting the contour plot on the xz plane, we can deduce that any significant alteration in x corresponds to an opposite change in the distribution's direction.
- All field variables adhere to the boundary constraints.

8 Conclusions

This research comprehensively analyzes the behavior of plane waves within a piezo-elastic medium subjected to hygro-thermal environments. Applying the rigorous mathematical approach of normal mode analysis, we reveal the nuanced dynamics of the thermo-piezo-elastic medium. Our examination sheds light on the interplay between moisture content, moisture diffusivity, and temperature
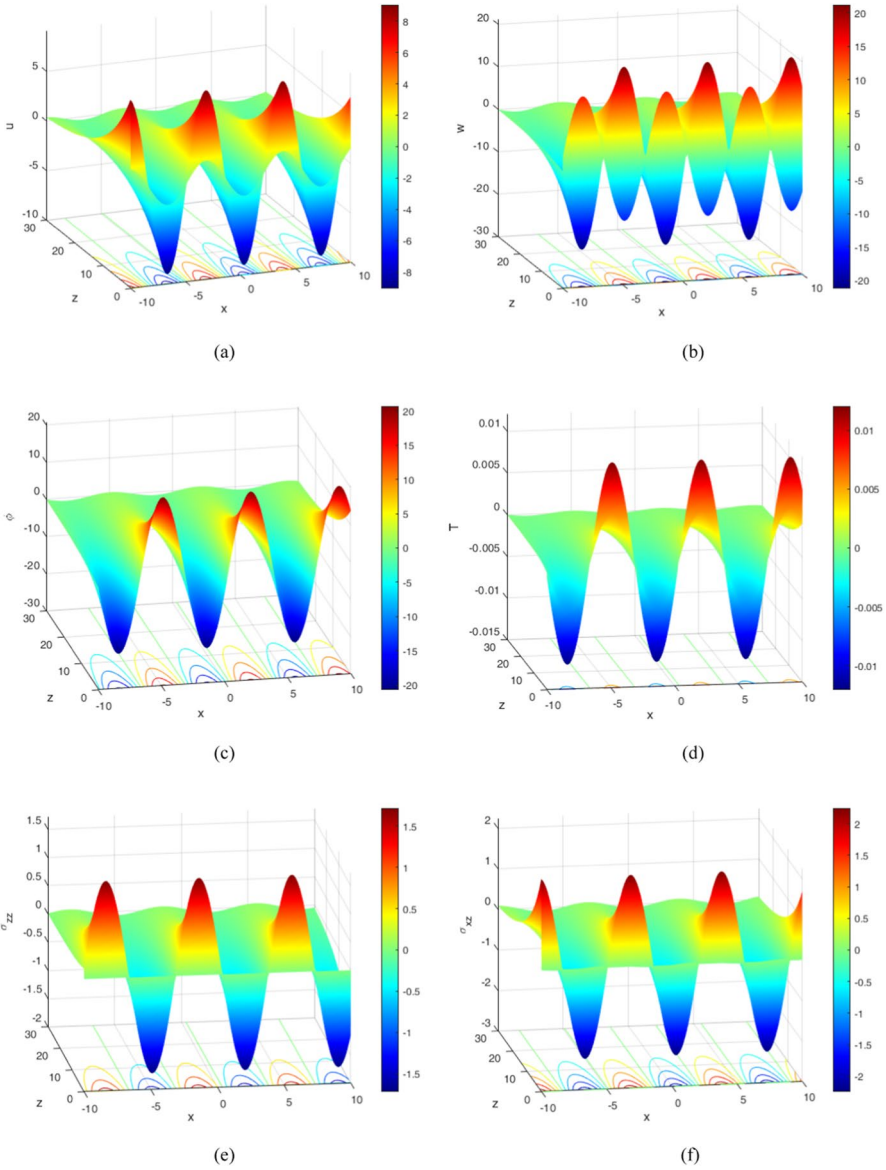
Fig. 5 a–i Distribution of the physical quantities in (x, z) plane when, $m_0 = 10\,\%, D_1^T = 50 \times 10^{-4}$, $D_3^T = 75 \times 10^{-4}, D_1^m = 0.8 \times 10^{-4}, D_3^m = 1.1 \times 10^{-4}$

diffusivity, which collectively shape the comprehensive physical field distribution of the CdSe material. Based on our detailed analysis, several notable outcomes emerge:
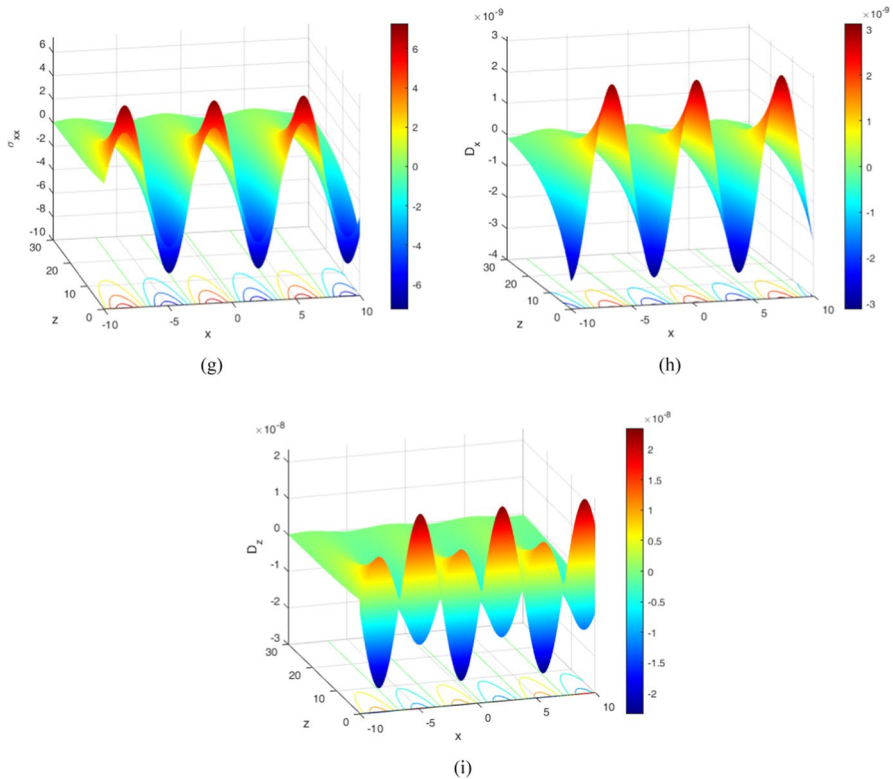
(g)

(h)

(i)

Fig. 5 (continued)

- The field variables' magnitudes decrease in the z direction, validating the assumption (24) and supporting previous research conducted by Mondal and Othman [48]. This phenomenon ensures the finite propagation speed of the thermal wave.
- All physical quantities in the system have both continuity and boundary condition agreements.
- The moisture content and moisture and temperature diffusivities significantly impact all the physical field distribution of the hygro-piezo-thermo-elastic model.
- The distribution of physical fields in the hygro-piezo-thermo-elastic model is notably influenced by moisture and temperature diffusivities. Importantly, these impacts do not exhibit a straightforward direct proportionality, adding a layer of complexity to the interplay between these factors
- The outcomes of this study contribute to enhancing the performance and durability of electronic devices, sensors, energy harvesting systems, materials for structural health monitoring, and infrastructure, particularly in the face of fluctuating moisture and temperature conditions.

Appendix

$$B_0 = Q_3^T c_{55} \eta_{33}^2 q_3^m - D_3^T D_3^m c_{55} \eta_{33}^2 - D_3^T D_3^m c_{33} c_{55} \varepsilon_{33} + Q_3^T c_{33} c_{55} \varepsilon_{33} q_3^m$$

$B_1 = (D_3^T a_{45} c_{55} \eta_{33}^2 - D_3^T D_3^m a_{11} \eta_{33}^2 + D_3^m a_{34} c_{55} \eta_{33}^2 - Q_3^T a_{35} c_{55} \eta_{33}^2 + Q_3^T a_{11} \eta_{33}^2 q_3^m - a_{44} c_{55} \eta_{33}^2 q_3^m - D_3^T D_3^m a_{13}$

$a_{51} c_{33} + D_3^T D_3^m a_{53} c_{33} c_{55} + D_3^T D_3^m a_{12} a_{21} \varepsilon_{33} + D_3^T D_3^m a_{13} a_{21} \eta_{33} + D_3^T D_3^m a_{12} a_{51} \eta_{33} - D_3^T D_3^m a_{11} c_{33}$

$\varepsilon_{33} + D_3^T D_3^m a_{22} c_{55} \varepsilon_{33} + D_3^T D_3^m a_{23} c_{55} \eta_{33} + D_3^T D_3^m a_{52} c_{55} \eta_{33} - D_3^T a_{43} c_{33} c_{55} d_3 + D_3^m a_{32} \beta_3^T c_{55} \varepsilon_{33}$

$+ D_3^T a_{42} \beta_3^m c_{55} \varepsilon_{33} - D_3^m a_{33} \beta_3^T c_{55} \eta_{33} - D_3^T a_{43} \beta_3^m c_{55} \eta_{33} + D_3^T a_{45} c_{33} c_{55} \varepsilon_{33} + D_3^m a_{34} c_{33} c_{55} \varepsilon_{33} - D_3^T$

$a_{42} c_{55} d_3 \eta_{33} + Q_3^T a_{33} c_{33} c_{55} d_3 - Q_3^T a_{32} \beta_3^m c_{55} \varepsilon_{33} + Q_3^T a_{33} \beta_3^m c_{55} \eta_{33} - Q_3^T a_{35} c_{33} c_{55} \varepsilon_{33} + Q_3^T a_{32} c_{55}$

$d_3 \eta_{33} - D_3^m a_{33} c_{33} c_{55} \tau_3 - D_3^m a_{32} c_{55} \eta_{33} \tau_3 + Q_3^T a_{13} a_{51} c_{33} q_3^m - Q_3^T a_{53} c_{33} c_{55} q_3^m - Q_3^T a_{12} a_{21} \varepsilon_{33} q_3^m - Q_3^T a_{13}$

$a_{21} \eta_{33} q_3^m - Q_3^T a_{12} a_{51} \eta_{33} q_3^m + Q_3^T a_{11} c_{33} \varepsilon_{33} q_3^m - Q_3^T a_{22} c_{55} \varepsilon_{33} q_3^m - Q_3^T a_{23} c_{55} \eta_{33} q_3^m - Q_3^T a_{52} c_{55} \eta_{33} q_3^m$

$- a_{42} \beta_3^T c_{55} \varepsilon_{33} q_3^m + a_{43} \beta_3^T c_{55} \eta_{33} q_3^m - a_{44} c_{33} c_{55} \varepsilon_{33} q_3^m + a_{43} c_{33} c_{55} q_3^m \tau_3 + a_{42} c_{55} \eta_{33} q_3^m \tau_3)/B_0$

$B_2 = (D_3^T a_{11} a_{45} \eta_{33}^2 - D_3^T a_{15} a_{41} \eta_{33}^2 + D_3^m a_{11} a_{34} \eta_{33}^2 - D_3^m a_{14} a_{31} \eta_{33}^2 - Q_3^T a_{11} a_{35} \eta_{33}^2 + Q_3^T a_{15} a_{31} \eta_{33}^2 - a_{34} a_{45}$

$c_{55} \eta_{33}^2 + a_{35} a_{44} c_{55} \eta_{33}^2 - a_{11} a_{44} \eta_{33}^2 q_3^m + D_3^m a_{14} a_{31} \eta_{33}^2 - Q_3^T a_{11} a_{35} \eta_{33}^2 + Q_3^T a_{15} a_{31} \eta_{33}^2 - a_{34} a_{45} c_{55} \eta_{33}^2$

$+ a_{35} a_{44} c_{55} \eta_{33}^2 - a_{11} a_{44} \eta_{33}^2 q_3^m + a_{14} a_{41} \eta_{33}^2 q_3^m - D_3^T D_3^m a_{12} a_{21} a_{53} - D_3^T D_3^m a_{12} a_{23} a_{51} - D_3^T D_3^m a_{13} a_{21}$

$a_{52} + D_3^T D_3^m a_{13} a_{22} a_{51} + D_3^T D_3^m a_{11} a_{53} c_{33} - D_3^T D_3^m a_{22} a_{53} c_{55} - D_3^T D_3^m a_{23} a_{52} c_{55} + D_3^T D_3^m a_{11} a_{22} \varepsilon_{33}$

$+ D_3^T D_3^m a_{11} a_{23} \eta_{33} + D_3^T D_3^m a_{11} a_{52} \eta_{33} + D_3^m a_{12} a_{33} a_{51} \beta_3^T + D_3^m a_{13} a_{32} a_{51} \beta_3^T + D_3^T a_{12} a_{43} a_{51} \beta_3^m$

$+ D_3^T a_{13} a_{42} a_{51} \beta_3^m + D_3^T a_{13} a_{45} a_{51} c_{33} - D_3^T a_{15} a_{43} a_{51} c_{33} + D_3^m a_{13} a_{34} a_{51} c_{33} - D_3^m a_{14} a_{33} a_{51} c_{33} +$

$D_3^T a_{12} a_{21} a_{43} d_3 + D_3^T a_{13} a_{21} a_{42} d_3 - D_3^m a_{32} a_{53} \beta_3^T c_{55} + D_3^m a_{33} a_{52} \beta_3^T c_{55} - D_3^T a_{42} a_{53} \beta_3^m c_{55} + D_3^T$

$a_{43} a_{52} \beta_3^m c_{55} - D_3^T a_{45} a_{53} c_{33} c_{55} - D_3^m a_{34} a_{53} c_{33} c_{55} - D_3^T a_{12} a_{21} a_{45} \varepsilon_{33} - D_3^T a_{15} a_{21} a_{42} \varepsilon_{33} - D_3^m a_{12} a_{21}$

$a_{34} \varepsilon_{33} - D_3^m a_{14} a_{21} a_{32} \varepsilon_{33} - D_3^T a_{13} a_{21} a_{45} \eta_{33} + D_3^T a_{15} a_{21} a_{43} \eta_{33} - D_3^m a_{13} a_{21} a_{34} \eta_{33} + D_3^m a_{14} a_{21} a_{33}$

$\eta_{33} - D_3^T a_{12} a_{45} a_{51} \eta_{33} - D_3^T a_{15} a_{42} a_{51} \eta_{33} - D_3^m a_{12} a_{34} a_{51} \eta_{33} - D_3^m a_{14} a_{32} a_{51} \eta_{33} - D_3^T a_{11} a_{43} c_{33} d_3 +$

$D_3^T a_{13} a_{41} c_{33} d_3 + D_3^T a_{22} a_{43} c_{55} d_3 + D_3^T a_{23} a_{42} c_{55} d_3 + D_3^m a_{11} a_{32} \beta_3^T \varepsilon_{33} + D_3^m a_{12} a_{31} \beta_3^T \varepsilon_{33} + D_3^T a_{11}$

$a_{42} \beta_3^m \varepsilon_{33} + D_3^T a_{12} a_{41} \beta_3^m \varepsilon_{33} - D_3^m a_{11} a_{33} \beta_3^T \eta_{33} + D_3^m a_{13} a_{31} \beta_3^T \eta_{33} - D_3^T a_{11} a_{43} \beta_3^m \eta_{33} + D_3^T a_{13} a_{41}$

$\beta_3^m \eta_{33} + D_3^T a_{11} a_{45} c_{33} \varepsilon_{33} - D_3^T a_{15} a_{41} c_{33} \varepsilon_{33} + D_3^m a_{11} a_{34} c_{33} \varepsilon_{33} - D_3^m a_{14} a_{31} c_{33} \varepsilon_{33} - D_3^T a_{22} a_{45} c_{55} \varepsilon_{33}$

$- D_3^m a_{22} a_{34} c_{55} \varepsilon_{33} - D_3^T a_{23} a_{45} c_{55} \eta_{33} - D_3^m a_{23} a_{34} c_{55} \eta_{33} - D_3^T a_{45} a_{52} c_{55} \eta_{33} - D_3^m a_{34} a_{52} c_{55} \eta_{33} - D_3^T a_{11}$

$a_{42} d_3 \eta_{33} - D_3^T a_{12} a_{41} d_3 \eta_{33} - Q_3^T a_{12} a_{33} a_{51} \beta_3^m - Q_3^T a_{13} a_{32} a_{51} \beta_3^m - Q_3^T a_{13} a_{35} a_{51} c_{33} + Q_3^T a_{15} a_{33} a_{51} c_{33}$

$- Q_3^T a_{12} a_{21} a_{33} d_3 - Q_3^T a_{13} a_{21} a_{32} d_3 + Q_3^T a_{32} a_{53} \beta_3^m c_{55} - Q_3^T a_{33} a_{52} \beta_3^m c_{55} + Q_3^T a_{35} a_{53} c_{33} c_{55} + Q_3^T a_{12}$

$a_{21} a_{35} \varepsilon_{33} + Q_3^T a_{15} a_{21} a_{32} \varepsilon_{33} + Q_3^T a_{13} a_{21} a_{35} \eta_{33} - Q_3^T a_{15} a_{21} a_{33} \eta_{33} + Q_3^T a_{12} a_{35} a_{51} \eta_{33} + Q_3^T a_{15} a_{32} a_{51}$

$\eta_{33} + Q_3^T a_{11} a_{33} c_{33} d_3 - Q_3^T a_{13} a_{31} c_{33} d_3 - Q_3^T a_{22} a_{33} c_{55} d_3 - Q_3^T a_{23} a_{32} c_{55} d_3 - Q_3^T a_{11} a_{32} \beta_3^m \varepsilon_{33} - Q_3^T a_{12}$

$a_{31} \beta_3^m \varepsilon_{33} + Q_3^T a_{11} a_{33} \beta_3^m \eta_{33} - Q_3^T a_{13} a_{31} \beta_3^m \eta_{33} + D_3^m a_{12} a_{21} a_{33} \tau_3 + D_3^m a_{13} a_{21} a_{32} \tau_3 - Q_3^T a_{11} a_{35} c_{33}$

$\varepsilon_{33} + Q_3^T a_{15} a_{31} c_{33} \varepsilon_{33} + Q_3^T a_{22} a_{35} c_{55} \varepsilon_{33} + Q_3^T a_{23} a_{35} c_{55} \eta_{33} + Q_3^T a_{35} a_{52} c_{55} \eta_{33} + Q_3^T a_{11} a_{32} d_3 \eta_{33} +$

$Q_3^T a_{12} a_{31} d_3 \eta_{33} - D_3^m a_{11} a_{33} c_{33} \tau_3 + D_3^m a_{13} a_{31} c_{33} \tau_3 + D_3^m a_{22} a_{33} c_{55} \tau_3 + D_3^m a_{23} a_{32} c_{55} \tau_3 -$

$D_3^m a_{11} a_{32} \eta_{33} \tau_3 - D_3^m a_{12} a_{31} \eta_{33} \tau_3 + Q_3^T a_{12} a_{21} a_{53} q_3^m + Q_3^T a_{12} a_{23} a_{51} q_3^m + Q_3^T a_{13} a_{21} a_{52} q_3^m - Q_3^T a_{13}$

$$a_{22}a_{51}q_3^m - Q_3^T a_{11}a_{53}c_{33}q_3^m + Q_3^T a_{22}a_{53}c_{55}q_3^m + Q_3^T a_{23}a_{52}c_{55}q_3^m - Q_3^T a_{11}a_{22}\varepsilon_{33}q_3^m - Q_3^T a_{11}a_{23}\eta_{33}$$

$$q_3^m - Q_3^T a_{11}a_{52}\eta_{33}q_3^m + a_{32}a_{43}\beta_3^T c_{55}d_3 - a_{33}a_{42}\beta_3^T c_{55}d_3 - a_{33}a_{44}c_{33}c_{55}d_3 + a_{34}a_{43}c_{33}c_{55}d_3 - a_{32}$$

$$a_{45}\beta_3^T c_{55}\varepsilon_{33} + a_{35}a_{42}\beta_3^T c_{55}\varepsilon_{33} + a_{32}a_{44}\beta_3^m c_{55}\varepsilon_{33} - a_{34}a_{42}\beta_3^m c_{55}\varepsilon_{33} + a_{33}a_{45}\beta_3^T c_{55}\eta_{33} - a_{35}a_{43}$$

$$\beta_3^T c_{55}\eta_{33} - a_{33}a_{44}\beta_3^m c_{55}\eta_{33} + a_{34}a_{43}\beta_3^m c_{55}\eta_{33} - a_{34}a_{45}c_{33}c_{55}\varepsilon_{33} + a_{35}a_{44}c_{33}c_{55}\varepsilon_{33} - a_{32}a_{44}c_{55}$$

$$d_3\eta_{33} + a_{34}a_{42}c_{55}d_3\eta_{33} - a_{12}a_{43}a_{51}\beta_3^T q_3^m - a_{13}a_{42}a_{51}\beta_3^T q_3^m - a_{13}a_{44}a_{51}c_{33}q_3^m + a_{14}a_{43}a_{51}c_{33}q_3^m$$

$$+a_{42}a_{53}\beta_3^T c_{55}q_3^m - a_{43}a_{52}\beta_3^T c_{55}q_3^m + a_{44}a_{53}c_{33}c_{55}q_3^m + a_{12}a_{21}a_{44}\varepsilon_{33}q_3^m + a_{14}a_{21}a_{42}\varepsilon_{33}q_3^m +$$

$$a_{13}a_{21}a_{44}\eta_{33}q_3^m - a_{14}a_{21}a_{43}\eta_{33}q_3^m + a_{12}a_{44}a_{51}\eta_{33}q_3^m + a_{14}a_{42}a_{51}\eta_{33}q_3^m - a_{11}a_{42}\beta_3^T\eta_{33}q_3^m - a_{12}$$

$$a_{41}\beta_3^T\varepsilon_{33}q_3^m + a_{11}a_{43}\beta_3^T\eta_{33}q_3^m - a_{13}a_{41}\beta_3^T\eta_{33}q_3^m - a_{11}a_{44}c_{33}\varepsilon_{33}q_3^m + a_{14}a_{41}c_{33}\varepsilon_{33}q_3^m + a_{22}a_{44}$$

$$c_{55}\varepsilon_{33}q_3^m + a_{23}a_{44}c_{55}\eta_{33}q_3^m + a_{44}a_{52}c_{55}\eta_{33}q_3^m - a_{32}a_{43}\beta_3^m c_{55}\tau_3 + a_{33}a_{42}\beta_3^m c_{55}\tau_3 + a_{33}a_{45}c_{33}$$

$$c_{55}\tau_3 - a_{35}a_{43}c_{33}c_{55}\tau_3 + a_{32}a_{45}c_{55}\eta_{33}\tau_3 - a_{35}a_{42}c_{55}\eta_{33}\tau_3 - a_{12}a_{21}a_{43}q_3^m\tau_3 - a_{13}a_{21}a_{42}q_3^m\tau_3 + a_{11}$$

$$a_{43}c_{33}q_3^m\tau_3 - a_{13}a_{41}c_{33}q_3^m\tau_3 - a_{22}a_{43}c_{55}q_3^m\tau_3 - a_{23}a_{42}c_{55}q_3^m\tau_3 + a_{11}a_{42}\eta_{33}q_3^m\tau_3 + a_{12}a_{41}\eta_{33}q_3^m\tau_3)/B_0$$

$$B_3 = ((-a_{11}a_{22}a_{53} - a_{11}a_{23}a_{52})D_3^T D_3^m + (a_{15}a_{23}a_{41} - a_{11}a_{23}a_{45} - a_{11}a_{45}a_{52} + a_{15}a_{41}a_{52})D_3^T\eta_{33} + (a_{15}$$

$$a_{22}a_{41} - a_{11}a_{22}a_{45})D_3^T\varepsilon_{33} + (a_{11}a_{43}a_{52} - a_{11}a_{42}a_{53} - a_{12}a_{41}a_{53} - a_{13}a_{41}a_{52})D_3^T\beta_3^m + (a_{12}a_{21}a_{45}a_{53}$$

$$+a_{12}a_{23}a_{45}a_{51} + a_{13}a_{21}a_{45}a_{52} - a_{13}a_{22}a_{45}a_{51} + a_{15}a_{21}a_{42}a_{53} - a_{15}a_{21}a_{43}a_{52} + a_{15}a_{22}a_{43}a_{51} + a_{15}$$

$$a_{23}a_{42}a_{51} - a_{11}a_{45}a_{53}c_{33} + a_{15}a_{41}a_{53}c_{33} + a_{22}a_{45}a_{53}c_{55} + a_{23}a_{45}a_{52}c_{55} + a_{11}a_{22}a_{43}d_3 + a_{11}a_{23}a_{42}$$

$$d_3 + a_{12}a_{23}a_{41}d_3 - a_{13}a_{22}a_{41}d_3)D_3^T + (a_{14}a_{23}a_{31} - a_{11}a_{23}a_{34} - a_{11}a_{34}a_{52} + a_{14}a_{31}a_{52})D_3^m\eta_{33} +$$

$$(a_{14}a_{22}a_{31} - a_{11}a_{22}a_{34})D_3^m\varepsilon_{33} + (a_{11}a_{33}a_{52} - a_{11}a_{32}a_{53} - a_{12}a_{31}a_{53} - a_{13}a_{31}a_{52})D_3^m\beta_3^T + (a_{11}a_{22}$$

$$a_{33} + a_{11}a_{23}a_{32} + a_{12}a_{23}a_{31} - a_{13}a_{22}a_{31})D_3^m\tau_3 + (a_{12}a_{21}a_{34}a_{53} + a_{12}a_{23}a_{34}a_{51} + a_{13}a_{21}a_{34}a_{52} -$$

$$a_{13}a_{22}a_{34}a_{51} + a_{14}a_{21}a_{32}a_{53} - a_{14}a_{21}a_{33}a_{52} + a_{14}a_{22}a_{33}a_{51} + a_{14}a_{23}a_{32}a_{51} - a_{11}a_{34}a_{53}c_{33} + a_{14}$$

$$a_{31}a_{53}c_{33} + a_{22}a_{34}a_{53}c_{55} + a_{23}a_{34}a_{52}c_{55})D_3^m + (a_{11}a_{35}a_{44} - a_{11}a_{34}a_{45} + a_{14}a_{31}a_{45} - a_{14}a_{35}a_{41} -$$

$$a_{15}a_{31}a_{44} + a_{15}a_{34}a_{41})\eta_{33}^2 + (a_{11}a_{34}a_{43} - a_{11}a_{33}a_{44} + a_{13}a_{31}a_{44} - a_{13}a_{34}a_{41} - a_{14}a_{31}a_{43} + a_{14}a_{33}$$

$$a_{41})\eta_{33}\beta_3^m + (a_{11}a_{33}a_{45} - a_{11}a_{35}a_{43} - a_{13}a_{31}a_{45} + a_{13}a_{35}a_{41} + a_{15}a_{31}a_{43} - a_{15}a_{33}a_{41})\eta_{33}\beta_3^T +$$

$$(a_{11}a_{32}a_{45} - a_{11}a_{35}a_{42} + a_{12}a_{31}a_{45} - a_{12}a_{35}a_{41} + a_{15}a_{31}a_{42} - a_{15}a_{32}a_{41})\eta_{33}\tau_3 + (Q_3^T a_{11}a_{23}a_{35} -$$

$$Q_3^T a_{15}a_{23}a_{31} + Q_3^T a_{11}a_{35}a_{52} - Q_3^T a_{15}a_{31}a_{52} + a_{13}a_{21}a_{34}a_{45} - a_{13}a_{21}a_{35}a_{44} - a_{14}a_{21}a_{33}a_{45} + a_{14}$$

$$a_{21}a_{35}a_{43} + a_{15}a_{21}a_{33}a_{44} - a_{15}a_{21}a_{34}a_{43} + a_{12}a_{34}a_{45}a_{51} - a_{12}a_{35}a_{44}a_{51} + a_{14}a_{32}a_{45}a_{51} - a_{14}a_{35}$$

$$a_{42}a_{51} - a_{15}a_{32}a_{44}a_{51} + a_{15}a_{34}a_{42}a_{51} + a_{23}a_{34}a_{45}c_{55} - a_{23}a_{35}a_{44}c_{55} + a_{34}a_{45}a_{52}c_{55} - a_{35}a_{44}a_{52}$$

$$c_{55} - a_{11}a_{32}a_{44}d_3 + a_{11}a_{34}a_{42}d_3 - a_{12}a_{31}a_{44}d_3 + a_{12}a_{34}a_{41}d_3 - a_{14}a_{31}a_{42}d_3 + a_{14}a_{32}a_{41}d_3 + a_{11}$$

$$a_{23}a_{44}q_3^m - a_{14}a_{23}a_{41}q_3^m + a_{11}a_{44}a_{52}q_3^m - a_{14}a_{41}a_{52}q_3^m)\eta_{33} + (a_{11}a_{32}a_{44} - a_{11}a_{34}a_{42} + a_{12}a_{31}a_{44}$$

$$-a_{12}a_{34}a_{41} + a_{14}a_{31}a_{42} - a_{14}a_{32}a_{41})\varepsilon_{33}\beta_3^m + (a_{11}a_{35}a_{42} - a_{11}a_{32}a_{45} - a_{12}a_{31}a_{45} + a_{12}a_{35}a_{41} -$$

$$a_{15}a_{31}a_{42} + a_{15}a_{32}a_{41})\varepsilon_{33}\beta_3^T + (Q_3^T a_{11}a_{22}a_{35} - Q_3^T a_{15}a_{22}a_{31} + a_{22}a_{34}a_{45}c_{55} - a_{22}a_{35}a_{44}c_{55} + a_{11}$$

$$a_{22}a_{44}q_3^m - a_{14}a_{22}a_{41}q_3^m)\varepsilon_{33} + (a_{11}a_{33}a_{42} - a_{11}a_{32}a_{43} - a_{12}a_{31}a_{43} + a_{12}a_{33}a_{41} - a_{13}a_{31}a_{42} + a_{13}$$

$$a_{32}a_{41})\beta_3^m\tau_3 + (Q_3^T a_{11}a_{32}a_{53} - Q_3^T a_{11}a_{33}a_{52} + Q_3^T a_{12}a_{31}a_{53} + Q_3^T a_{13}a_{31}a_{52} + a_{12}a_{33}a_{44}a_{51} - a_{12}$$

$$a_{34}a_{43}a_{51} + a_{13}a_{32}a_{44}a_{51} - a_{13}a_{34}a_{42}a_{51} - a_{14}a_{32}a_{43}a_{51} + a_{14}a_{33}a_{42}a_{51} - a_{32}a_{44}a_{53}c_{55} + a_{33}a_{44}$$

$$a_{52}c_{55} + a_{34}a_{42}a_{53}c_{55} - a_{34}a_{43}a_{52}c_{55})\beta_3^m + (a_{12}a_{35}a_{43}a_{51} - a_{12}a_{33}a_{45}a_{51} - a_{13}a_{32}a_{45}a_{51} + a_{13}$$
$$a_{35}a_{42}a_{51} + a_{15}a_{32}a_{43}a_{51} - a_{15}a_{33}a_{42}a_{51} + a_{32}a_{45}a_{53}c_{55} - a_{33}a_{45}a_{52}c_{55} - a_{35}a_{42}a_{53}c_{55} + a_{13}$$
$$a_{35}a_{42}a_{51} + a_{15}a_{32}a_{43}a_{51} - a_{15}a_{33}a_{42}a_{51} + a_{32}a_{45}a_{53}c_{55} - a_{33}a_{45}a_{52}c_{55} - a_{35}a_{42}a_{53}c_{55} + a_{35}$$
$$a_{43}a_{52}c_{55} + a_{11}a_{32}a_{43}d_3 - a_{11}a_{33}a_{42}d_3 + a_{12}a_{31}a_{43}d_3 - a_{12}a_{33}a_{41}d_3 + a_{13}a_{31}a_{42}d_3 - a_{13}a_{32}$$
$$a_{41}d_3 + a_{11}a_{42}a_{53}q_3^m - a_{11}a_{43}a_{52}q_3^m + a_{12}a_{41}a_{53}q_3^m + a_{13}a_{41}a_{52}q_3^m)\beta_3^T + (a_{12}a_{21}a_{35}a_{43} -$$
$$a_{12}a_{21}a_{33}a_{45} - a_{13}a_{21}a_{32}a_{45} + a_{13}a_{21}a_{35}a_{42} + a_{15}a_{21}a_{32}a_{43} - a_{15}a_{21}a_{33}a_{42} + a_{11}a_{33}a_{45}c_{33}$$
$$-a_{11}a_{35}a_{43}c_{33} - a_{13}a_{31}a_{45}c_{33} + a_{13}a_{35}a_{41}c_{33} + a_{15}a_{31}a_{43}c_{33} - a_{15}a_{33}a_{41}c_{33} - a_{22}a_{33}a_{45}c_{55}$$
$$+a_{22}a_{35}a_{43}c_{55} - a_{23}a_{32}a_{45}c_{55} + a_{23}a_{35}a_{42}c_{55} - a_{11}a_{22}a_{43}q_3^m - a_{11}a_{23}a_{42}q_3^m - a_{12}a_{23}a_{41}q_3^m +$$
$$a_{13}a_{22}a_{41}q_3^m)\tau_3 + Q_3^T a_{13}a_{22}a_{35}a_{51} - Q_3^T a_{12}a_{23}a_{35}a_{51} - Q_3^T a_{13}a_{21}a_{35}a_{52} - Q_3^T a_{12}a_{21}a_{35}a_{53} -$$
$$Q_3^T a_{15}a_{21}a_{32}a_{53} + Q_3^T a_{15}a_{21}a_{33}a_{52} - Q_3^T a_{15}a_{22}a_{33}a_{51} - Q_3^T a_{15}a_{23}a_{32}a_{51} + Q_3^T a_{11}a_{35}a_{53}c_{33}$$
$$-Q_3^T a_{15}a_{31}a_{53}c_{33} - Q_3^T a_{22}a_{35}a_{53}c_{55} - Q_3^T a_{23}a_{35}a_{52}c_{55} - Q_3^T a_{11}a_{22}a_{33}d_3 - Q_3^T a_{11}a_{23}a_{32}d_3 -$$
$$Q_3^T a_{12}a_{23}a_{31}d_3 + Q_3^T a_{13}a_{22}a_{31}d_3 + Q_3^T a_{11}a_{22}a_{53}q_3^m + Q_3^T a_{11}a_{23}a_{52}q_3^m - a_{13}a_{34}a_{45}a_{51}c_{33}$$
$$+a_{13}a_{35}a_{44}a_{51}c_{33} + a_{14}a_{33}a_{45}a_{51}c_{33} - a_{14}a_{35}a_{43}a_{51}c_{33} - a_{15}a_{33}a_{44}a_{51}c_{33} + a_{15}a_{34}a_{43}a_{51}c_{33}$$
$$+a_{12}a_{21}a_{33}a_{44}d_3 - a_{12}a_{21}a_{34}a_{43}d_3 + a_{13}a_{21}a_{32}a_{44}d_3 - a_{13}a_{21}a_{34}a_{42}d_3 - a_{14}a_{21}a_{32}a_{43}d_3 +$$
$$a_{14}a_{21}a_{33}a_{42}d_3 + a_{34}a_{45}a_{53}c_{33}c_{55} - a_{35}a_{44}a_{53}c_{33}c_{55} - a_{11}a_{33}a_{44}c_{33}d_3 + a_{11}a_{34}a_{43}c_{33}d_3 +$$
$$a_{13}a_{31}a_{44}c_{33}d_3 - a_{13}a_{34}a_{41}c_{33}d_3 - a_{14}a_{31}a_{43}c_{33}d_3 + a_{14}a_{33}a_{41}c_{33}d_3 + a_{22}a_{33}a_{44}c_{55}d_3 - a_{22}$$
$$a_{34}a_{43}c_{55}d_3 + a_{23}a_{32}a_{44}c_{55}d_3 - a_{23}a_{34}a_{42}c_{55}d_3 + (-a_{12}a_{21}a_{44}a_{53} - a_{12}a_{23}a_{44}a_{51} - a_{13}a_{21}$$
$$a_{44}a_{52} + a_{13}a_{22}a_{44}a_{51} - a_{14}a_{21}a_{42}a_{53} + a_{14}a_{21}a_{43}a_{52} - a_{14}a_{22}a_{43}a_{51} - a_{14}a_{23}a_{42}a_{51} + a_{11}$$
$$a_{44}a_{53}c_{33} - a_{14}a_{41}a_{53}c_{33} - a_{22}a_{44}a_{53}c_{55} - a_{23}a_{44}a_{52}c_{55})q_3^m)/B_0$$

$$B_4 = ((a_{11}a_{22}a_{45}a_{53} + a_{11}a_{23}a_{45}a_{52} - a_{15}a_{22}a_{41}a_{53} - a_{15}a_{23}a_{41}a_{52})D_3^T + (a_{11}a_{22}a_{34}a_{53} + a_{11}a_{23}$$
$$a_{34}a_{52} - a_{14}a_{22}a_{31}a_{53} - a_{14}a_{23}a_{31}a_{52})D_3^m + (a_{11}a_{23}a_{34}a_{45} - a_{11}a_{23}a_{35}a_{44} - a_{14}a_{23}a_{31}a_{45} + a_{14}$$
$$a_{23}a_{35}a_{41} + a_{15}a_{23}a_{31}a_{44} - a_{15}a_{23}a_{34}a_{41} + a_{11}a_{34}a_{45}a_{52} - a_{11}a_{35}a_{44}a_{52} - a_{14}a_{31}a_{45}a_{52} + a_{14}$$
$$a_{35}a_{41}a_{52} + a_{15}a_{31}a_{44}a_{52} - a_{15}a_{34}a_{41}a_{52})\eta_{33} + (a_{11}a_{22}a_{34}a_{45} - a_{11}a_{22}a_{35}a_{44} - a_{14}a_{22}a_{31}a_{45}$$
$$+a_{14}a_{22}a_{35}a_{41} + a_{15}a_{22}a_{31}a_{44} - a_{15}a_{22}a_{34}a_{41})\varepsilon_{33} + (a_{11}a_{33}a_{44}a_{52} - a_{11}a_{32}a_{44}a_{53} + a_{11}a_{34}a_{42}$$
$$a_{53} - a_{11}a_{34}a_{43}a_{52} - a_{12}a_{31}a_{44}a_{53} + a_{12}a_{34}a_{41}a_{53} - a_{13}a_{31}a_{44}a_{52} + a_{13}a_{34}a_{41}a_{52} - a_{14}a_{31}a_{42}$$
$$a_{53} + a_{14}a_{31}a_{43}a_{52} + a_{14}a_{32}a_{41}a_{53} - a_{14}a_{33}a_{41}a_{52})\beta_3^m + (a_{11}a_{32}a_{45}a_{53} - a_{11}a_{33}a_{45}a_{52} - a_{11}$$
$$a_{35}a_{42}a_{53} + a_{11}a_{35}a_{43}a_{52} + a_{12}a_{31}a_{45}a_{53} - a_{12}a_{35}a_{41}a_{53} + a_{13}a_{31}a_{45}a_{52} - a_{13}a_{35}a_{41}a_{52} + a_{15}$$
$$a_{31}a_{42}a_{53} - a_{15}a_{31}a_{43}a_{52} - a_{15}a_{32}a_{41}a_{53} + a_{15}a_{33}a_{41}a_{52})\beta_3^T + (a_{11}a_{22}a_{35}a_{43} - a_{11}a_{22}a_{33}a_{45}$$
$$-a_{11}a_{23}a_{32}a_{45} + a_{11}a_{23}a_{35}a_{42} - a_{12}a_{23}a_{31}a_{45} + a_{12}a_{23}a_{35}a_{41} + a_{13}a_{22}a_{31}a_{45} - a_{13}a_{22}a_{35}a_{41}$$
$$-a_{15}a_{22}a_{31}a_{43} + a_{15}a_{22}a_{33}a_{41} - a_{15}a_{23}a_{31}a_{42} + a_{15}a_{23}a_{32}a_{41})\tau_3 + (a_{15}a_{22}a_{31}a_{53} - a_{11}a_{23}a_{35}a_{52}$$
$$-a_{11}a_{22}a_{35}a_{53} + a_{15}a_{23}a_{31}a_{52})Q_3^T - a_{12}a_{21}a_{34}a_{45}a_{53} + a_{12}a_{21}a_{35}a_{44}a_{53} - a_{12}a_{23}a_{34}a_{45}a_{51} + a_{12}$$
$$a_{23}a_{35}a_{44}a_{51} - a_{13}a_{21}a_{34}a_{45}a_{52} + a_{13}a_{21}a_{35}a_{44}a_{52} + a_{13}a_{22}a_{34}a_{45}a_{51} - a_{13}a_{22}a_{35}a_{44}a_{51} - a_{14}a_{21}$$
$$a_{32}a_{45}a_{53} + a_{14}a_{21}a_{33}a_{45}a_{52} + a_{14}a_{21}a_{35}a_{42}a_{53} - a_{14}a_{21}a_{35}a_{43}a_{52} - a_{14}a_{22}a_{33}a_{45}a_{51} + a_{14}a_{22}a_{35}$$
$$a_{43}a_{51} - a_{14}a_{23}a_{32}a_{45}a_{51} + a_{14}a_{23}a_{35}a_{42}a_{51} + a_{15}a_{21}a_{32}a_{44}a_{53} - a_{15}a_{21}a_{33}a_{44}a_{52} - a_{15}a_{21}a_{34}a_{42}a_{53}$$
$$+a_{15}a_{21}a_{34}a_{43}a_{52} + a_{15}a_{22}a_{33}a_{44}a_{51} - a_{15}a_{22}a_{34}a_{43}a_{51} + a_{15}a_{23}a_{32}a_{44}a_{51} - a_{15}a_{23}a_{34}a_{42}a_{51} + a_{11}$$

$$a_{34}a_{45}a_{53}c_{33} - a_{11}a_{35}a_{44}a_{53}c_{33} - a_{14}a_{31}a_{45}a_{53}c_{33} + a_{14}a_{35}a_{41}a_{53}c_{33} + a_{15}a_{31}a_{44}a_{53}c_{33} - a_{15}a_{34}$$

$$a_{41}a_{53}c_{33} - a_{22}a_{34}a_{45}a_{53}c_{55} + a_{22}a_{35}a_{44}a_{53}c_{55} - a_{23}a_{34}a_{45}a_{52}c_{55} + a_{23}a_{35}a_{44}a_{52}c_{55} + a_{11}a_{22}$$

$$a_{33}a_{44}d_3 - a_{11}a_{22}a_{34}a_{43}d_3 + a_{11}a_{23}a_{32}a_{44}d_3 - a_{11}a_{23}a_{34}a_{42}d_3 + a_{12}a_{23}a_{31}a_{44}d_3 - a_{12}a_{23}a_{34}a_{41}$$

$$d_3 - a_{13}a_{22}a_{31}a_{44}d_3 + a_{13}a_{22}a_{34}a_{41}d_3 + a_{14}a_{22}a_{31}a_{43}d_3 - a_{14}a_{22}a_{33}a_{41}d_3 + a_{14}a_{23}a_{31}a_{42}d_3$$

$$-a_{14}a_{23}a_{32}a_{41}d_3 + (a_{14}a_{22}a_{41}a_{53} - a_{11}a_{22}a_{44}a_{53} - a_{11}a_{23}a_{44}a_{52} + a_{14}a_{23}a_{41}a_{52})q_3^m)/B_0$$

$$B_5 = (-a_{11}a_{22}a_{34}a_{45}a_{53} + a_{11}a_{22}a_{35}a_{44}a_{53} - a_{11}a_{23}a_{34}a_{45}a_{52} + a_{11}a_{23}a_{35}a_{44}a_{52} + a_{14}a_{22}a_{31}a_{45}a_{53} - a_{14}$$

$$a_{22}a_{35}a_{41}a_{53} + a_{14}a_{23}a_{31}a_{45}a_{52} - a_{14}a_{23}a_{35}a_{41}a_{52} - a_{15}a_{22}a_{31}a_{44}a_{53} + a_{15}a_{22}a_{34}a_{41}a_{53} - a_{15}a_{23}a_{31}$$

$$a_{44}a_{52} + a_{15}a_{23}a_{34}a_{41}a_{52})/B_0$$

Data Availability Data will be provided on request to the corresponding author.

Declarations

Conflict of interest The authors declare no conflict of interest.

Ethical approval All the authors demonstrating that they have adhered to the accepted ethical standards of a genuine research study.

Consent to participate Being the corresponding author, I have consent to participate of all the authors in this research work.

Consent to publish All the authors are agreed to publish this research work.

References

1. Smith, R.C.: Smart Material Systems. Society for Industrial and Applied Mathematics, Philadelphia (2005)
2. Sih, G.C., Michopoulos, J.G., Chou, S.C.: Hygrothermoelasticity. Springer, Netherlands, Dordrecht (1986)

3. Alhashash, A., Elidy, E.S., El-Bary, A.A., Tantawi, R.S., Lotfy, K.: Two-temperature semiconductor model photomechanical and thermal wave responses with moisture diffusivity process. Crystals (2022). https://doi.org/10.3390/cryst12121770

4. Alenazi, A., Ahmed, A., El-Bary, A.A., Tantawi, R.S., Lotfy, K.: Moisture photo-thermoelasticity diffusivity in semiconductor materials: a novel stochastic model. Crystals **13**(1), 1–25 (2023). https://doi.org/10.3390/cryst13010042

5. El-Sapa, S., Lotfy, K., Elidy, E.S., El-Bary, A., Tantawi, R.S.: Photothermal excitation process in semiconductor materials under the effect moisture diffusivity. SILICON (2023). https://doi.org/10.1007/s12633-023-02311-y

6. Curie, J., Curie, P.: Development by compression of polar electricity in hemihedral crystals with slanted faces'. Bull. Mineral. Soc. Fr. **3**(4), 90–93 (1880). https://doi.org/10.3406/bulmi.1880.1564

7. Mindlin, R.D.: Equations of high frequency vibrations of thermopiezoelectric crystal plates. Int. J. Solids Struct. **10**(6), 625–637 (1974). https://doi.org/10.1016/0020-7683(74)90047-X

8. Nowacki, W.: Some general theorems of thermopiezoelectricity. J. Therm. Stress. **1**(2), 171–182 (1978). https://doi.org/10.1080/01495737808926940

9. Nowacki, W. Foundation of linear piezoelectricity. In: Parkus, H. (ed) Electro-magnetic Interactions in Elastic Solids. Chapter 1. Springer, Wein (1979)

10. Sharma, K., Marin, M.: Effect of distinct conductive and thermodynamic temperatures on the reflection of plane waves in micropolar elastic half-space. UPB Sci. Bull. Ser. A Appl. Math. Phys. **75**(2), 121–132 (2013)

11. Marin, M., Codarcea, L., Chirila, A.: Qualitative results on mixed problem of micropolar bodies with microtemperatures. Appl. Appl. Math. An Int. J. **12**(2), 9 (2017)

12. Lotfy, K.: Waves propagation for magneto-thermoelastic medium during the two-temperature theory with the gravitational field. Waves Random Complex Media (2022). https://doi.org/10.1080/17455030.2022.2122629

13. Gupta, V., Barak, M.S.: Quasi-P wave through orthotropic piezo-thermoelastic materials subject to higher order fractional and memory-dependent derivatives. Mech. Adv. Mater. Struct. (2023). https://doi.org/10.1080/15376494.2023.2217420

14. Gupta, V., Barak, M.S., Das, S.: Vibrational analysis of size-dependent thermo-piezo-photo-electric semiconductor medium under memory-dependent Moore–Gibson–Thompson photo-thermoelasticity theory. Mech. Adv. Mater. Struct. (2023). https://doi.org/10.1080/15376494.2023.2291804

15. Gupta, V., Barak, M.S., Ahmad, H.: Reflection of quasi plasma wave in photo-piezo semiconductor medium with distinct higher order fractional derivative two temperature models. Phys. Scr. (2023). https://doi.org/10.1088/1402-4896/ad1972

16. Barak, M.S., Kumar, R., Kumar, R., Gupta, V.: Energy transfer at the interface of monoclinic piezo-thermoelastic and thermoelastic half spaces with MDD. J. Therm. Stress. (2023). https://doi.org/10.1080/01495739.2023.2253879

17. Gupta, V., Barak, M.S.: Photo-thermo-piezo-elastic waves in semiconductor medium subject to distinct two temperature models with higher order memory dependencies. Int. J. Numer. Methods Heat Fluid Flow **34**(1), 84–108 (2024). https://doi.org/10.1108/HFF-07-2023-0380

18. Barak, M.S., et al.: Behavior of higher-order MDD on energy ratios at the interface of thermoelastic and piezothermoelastic mediums. Sci. Rep. **13**(1), 17170 (2023). https://doi.org/10.1038/s41598-023-44339-5

19. Kumar, R., Gupta, V., Pathania, V., Kumar, R., Barak, M.S.: Analysis of waves at boundary surfaces at distinct media with nonlocal dual-phase-lag. Proc. Natl. Acad. Sci. India Sect. A Phys. Sci. (2023). https://doi.org/10.1007/s40010-023-00850-y

20. Kumar, R., Gupta, V., Pathania, V., Barak, M.S.: Energy ratio response at the interface of elastic and dual-porous thermoelastic half-spaces. Phys. Scr. **98**(11), 115211 (2023). https://doi.org/10.1088/1402-4896/acfced

21. Kumar, R., Pathania, V., Gupta, V., Barak, M.S., Ahmad, H.: Thermoelastic modeling with dual porosity interacting with an inviscid liquid. J. Appl. Comput. Mech. **10**(1), 111–124 (2024). https://doi.org/10.22055/jacm.2023.44488.4221

22. Kumar, S., Barak, M.S., Kumari, N., Gupta, V., Ahmad, H.: The effect of viscosity and hyperbolic two-temperature on energy ratios in elastic and piezoviscothermoelastic half-spaces. Mech. Time-Dependent Mater. (2024). https://doi.org/10.1007/s11043-023-09657-1

23. Gupta, S., Das, S., Dutta, R., Verma, A.K.: Higher-order fractional and memory response in nonlocal double poro-magneto-thermoelastic medium with temperature-dependent properties excited by laser pulse. J. Ocean Eng. Sci. (2022). https://doi.org/10.1016/j.joes.2022.04.013

24. Gupta, S., Dutta, R., Das, S., Verma, A.K.: Double poro-magneto-thermoelastic model with micro-temperatures and initial stress under memory-dependent heat transfer. J. Therm. Stress. **46**(8), 743–774 (2023). https://doi.org/10.1080/01495739.2023.2202718

25. Dutta, R., Das, S., Bhengra, N., Vishwakarma, S.K., Das, S.K.: Nonlocal effect on shear wave propagation in a fiber-reinforced poroelastic layered structure subjected to interfacial impulsive disturbance. Soil Dyn. Earthq. Eng. **176**, 108307 (2024). https://doi.org/10.1016/j.soildyn.2023.108307

26. Raja, S., Sinha, P.K., Prathap, G., Dwarakanathan, D.: Influence of active stiffening on dynamic behaviour of piezo-hygro-thermo-elastic composite plates and shells. J. Sound Vib. **278**(1–2), 257–283 (2004). https://doi.org/10.1016/j.jsv.2003.10.002

27. Gupta, V., Sharma, M., Thakur, N.: Mathematical modeling of actively controlled piezo smart structures: a review. Smart Struct. Syst. **8**(3), 275–302 (2011). https://doi.org/10.12989/sss.2011.8.3.275

28. Zenkour, A.M., Alghanmi, R.A.: Hygro-thermo-electro-mechanical bending analysis of sandwich plates with FG core and piezoelectric faces. Mech. Adv. Mater. Struct. **28**(3), 282–294 (2021). https://doi.org/10.1080/15376494.2018.1562134

29. Tiwari, R., Mukhopadhyay, S.: On electromagneto-thermoelastic plane waves under Green-Naghdi theory of thermoelasticity-II. J. Therm. Stress. **40**(8), 1040–1062 (2017)

30. Tiwari, R., Mukhopadhyay, S.: Analysis of wave propagation in the presence of a continuous line heat source under heat transfer with memory dependent derivatives. Math. Mech. Solids **23**(5), 820–834 (2018)

31. Tiwari, R., Kumar, R., Abouelregal, A. E.: Analysis of a magneto-thermoelastic problem in a piezoelastic medium using the non-local memory-dependent heat conduction theory involving three phase lags. Mech. Time-Dependent Mater. 1–17 (2021).

32. Tiwari, R., Misra, J.C., Prasad, R.: Magneto-thermoelastic wave propagation in a finitely conducting medium: a comparative study for three types of thermoelasticity I, II, and III. J. Therm. Stress. **44**(7), 785–806 (2021)

33. Tiwari, R., Misra, J.C.: Magneto-thermoelastic excitation induced by a thermal shock: a study under the purview of three phase lag theory. Waves Random Complex Media **32**(2), 797–818 (2022)

34. Kumar, R., Tiwari, R., Singhal, A.: Analysis of the photo-thermal excitation in a semiconducting medium under the purview of DPL theory involving non-local effect. Meccanica **57**(8), 2027–2041 (2022)

35. Tiwari, R., Saeed, A.M., Kumar, R., Kumar, A., Singhal, A.: Memory response on generalized thermoelastic medium in context of dual phase lag thermoelasticity with non-local effect. Arch. Mech. **74**(2–3), 69–88 (2022)

36. Kaur, I., Singh, K., Ghita, G. M. D.: New analytical method for dynamic response of thermoelastic damping in simply supported generalized piezothermoelastic nanobeam. *ZAMM J. Appl. Math. Mech. Zeitschrift für Angew. Math. und Mech.* (2021). https://doi.org/10.1002/zamm.202100108

37. Kaur, I., Lata, P., Singh, K.: Thermoelastic damping in generalized simply supported piezo-thermoelastic nanobeam. Struct. Eng. Mech. **81**(1), 29–37 (2022)

38. Kaur, I., Singh, K., Ghita, G.M.D., Craciun, E.-M.: Modeling of a magneto-electro-piezo-thermoelastic nanobeam with two temperature subjected to ramp type heating. Proc. Rom. Acad. Ser. A **23**, 141–149 (2022)

39. Singh, K., Kaur, I., Craciun, E.-M.: Hygro-photo-thermoelastic solid cylinder under moisture and thermal diffusivity with Moore–Gibson–Thompson theory. Discov. Mech. Eng. **2**(1), 21 (2023). https://doi.org/10.1007/s44245-023-00028-1

40. Yadav, A.K., Carrera, E., Marin, M., Othman, M.I.A.: Reflection of hygrothermal waves in a Nonlocal Theory of coupled thermo-elasticity. Mech. Adv. Mater. Struct. (2022). https://doi.org/10.1080/15376494.2022.2130484

41. Barak, M.S., Gupta, V.: Memory-dependent and fractional order analysis of the initially stressed piezo-thermoelastic medium. Mech. Adv. Mater. Struct. (2023). https://doi.org/10.1080/15376494.2023.2211065

42. Szekeres, A.: Analogy between heat and moisture thermo-hygro-mechanical tailoring of composites by taking into account the second sound phenomenon. Comput. Struct. **76**(1), 145–152 (2000). https://doi.org/10.1016/S0045-7949(99)00170-4

43. Szekeres, A.: Cross-coupled heat and moisture transport: Part 1-theory. J. Therm. Stress. **35**(1–3), 248–268 (2012). https://doi.org/10.1080/01495739.2012.637827

44. Hosseini, S.M., Ghadiri Rad, M.H.: Application of meshless local integral equations for two-dimensional transient coupled hygrothermoelasticity analysis: moisture and thermoelastic wave propagations under shock loading. J. Therm. Stress. **40**(1), 40–54 (2017). https://doi.org/10.1080/01495739.2016.1224134

45. Ahmed, E.A.A., Abou-Dina, M.S., Ghaleb, A.F.: Plane wave propagation in a piezo-thermoelastic rotating medium within the dual-phase-lag model. Microsyst. Technol. **26**(3), 969–979 (2020). https://doi.org/10.1007/s00542-019-04567-0

46. Dutta, R., Das, S., Gupta, S., Singh, A., Chaudhary, H.: Nonlocal fiber-reinforced double porous material structure under fractional-order heat and mass transfer. Int. J. Numer. Methods Heat Fluid Flow **33**(11), 3608–3641 (2023). https://doi.org/10.1108/HFF-05-2023-0295

47. Yadav, A.K., Barak, M.S., Gupta, V.: Reflection at the free surface of the orthotropic piezo-hygro-thermo-elastic medium. Int. J. Numer. Methods Heat Fluid Flow (2023). https://doi.org/10.1108/HFF-04-2023-0208

48. Mondal, S., Othman, M.I.A.: Memory dependent derivative effect on generalized piezo-thermoelastic medium under three theories. Waves Random Complex Media **31**(6), 2150–2167 (2021). https://doi.org/10.1080/17455030.2020.1730480